Clinical descriptors of disease trajectories in patients with traumatic brain injury in the intensive care unit (CENTER-TBI): a multicentre observational cohort study

Cecilia A. I. Åkerlund[1,2] MD, Professor Anders Holst[2] PhD, Shubhayu Bhattacharyay[3] MSc, Professor Nino Stocchetti[4,5], Professor Ewout Steyerberg[6] PhD, Peter Smielewski[7] PhD, Professor David K. Menon[3] PhD, Ari Ercole[3,8] PhD, David W. Nelson[1] PhD and the CENTER-TBI participants and investigators[9]

[1] Section of Anaesthesiology and Intensive Care, Department of Physiology and Pharmacology, Karolinska Institutet, Stockholm, Sweden.

[2] School of Electrical Engineering and Computer Science, KTH Royal Institute of Technology, Stockholm, Sweden.

[3] Division of Anaesthesia, Department of Medicine, University of Cambridge, Cambridge, UK.

[4] Department of Physiopathology and Transplant, Milan University, Milan, Italy.

[5] Fondazione IRCCS Cà Granda Ospedale Maggiore Policlinico, Milan, Italy.

[6] Department of Biomedical Data Sciences, Leiden University Medical Center, Leiden, The Netherlands.

[7] Clinical Neuroscience, University of Cambridge, Cambridge, UK.

[8] Centre for Artificial Intelligence in Medicine, University of Cambridge, Cambridge, UK.

[9] A full list of the participants is provided in the acknowledgements

22 Correspondence to: David W Nelson, Function Perioperative Medicine and Intensive Care, Karolinska
23 University Hospital Solna, 171 76 Stockholm, david.nelson@regionstockholm.se, phone no
24 +46851779168

Word count: 3523. Abstract word count: 410.

Abstract

Background

Patients with traumatic brain injury (TBI) are a heterogeneous population, and the most severely injured individuals are often treated in an intensive care unit (ICU). The primary injury at impact, and the secondary insults that occur during the first week of the ICU stay, will affect outcome in this vulnerable group of patients. We aimed to identify clinical variables distinguishing disease trajectories among patients with traumatic brain injury admitted to the ICU.

Methods

We included patients with TBI who were admitted to the ICU at centres participating in the European multinational prospective observational Collaborative NeuroTrauma Effectiveness Research in TBI (CENTER-TBI) study, ranging from large academic to smaller rural hospitals. For every patient, we obtained pre-injury data and injury features, clinical characteristics on admission, demographics, physiological parameters, laboratory features, brain biomarkers (S100B, NSE, NFL, tau, UCH-L1 and GFAP), and ICP lowering treatments during the first 7 days of ICU stay. To identify temporal clinical disease trajectories, we applied a novel clustering method to these data, which was based on a mixture of probabilistic graph models with a Markov chain extension. The relation of clusters to the Glasgow Outcome Scale (GOS-E) was investigated.

Findings

We included 1728 patients with TBI. We found that glucose variation (defined as the difference between daily maximum and minimum glucose concentrations) and brain biomarkers (S100B, NSE, NFL, tau, UCH-L1 and GFAP) were consistently the main clinical descriptors of disease trajectories (defined as the leading variables contributing to and distinguishing clusters) in TBI patients in the ICU. Although information related to patient's outcome was not included in the clustering analysis,

different disease trajectories had different outcome profiles. Trajectory membership (to which cluster a patient is assigned in a model) was analysed as a predictor together with the variables of the IMPACT model and improved prediction of both mortality, and unfavourable outcome (dichotomized GOS-E levels < 5), increasing Nagelkerke's R^2 with 0·09 (from 0·44 to 0·53 and 0·36 to 0·45, respectively).

Interpretation

First day ICU admission variables are not the only clinical descriptors of disease trajectories in patients with TBI. With the addition of temporal variables in our study, variation of glucose was identified as the most important descriptor of disease trajectories in the ICU, which should motivate further research. Biomarkers of brain injury were consistently found to be top descriptors over time, suggesting they may be important in future clinical practice.

Funding

European Union 7th Framework program, Hannelore Kohl Stiftung, OneMind, Integra LifeSciences Corporation and NeuroTrauma Sciences.

Introduction

Patients with traumatic brain injury (TBI) treated in an intensive care unit (ICU) are extensively monitored and treated to minimise the risk of harmful secondary events. Thirty to forty percent of patients with severe TBI deteriorate within ten days post-injury.[1] A fundamental question in neurointensive care is how to monitor, identify and avoid secondary insult and further brain injury. Unfortunately, TBI patients are a highly heterogeneous patient group regarding their initial presentation and subsequent clinical trajectory or course. A recently published review[2] could only identify two studies classifying subgroups of patients with severe TBI in the acute phase, based on pre-injury and admission data, and it is unclear how these variables can be implemented into clinical practice.

In a previous study, we identified six distinct pathophysiological subgroups—so-called endotypes—of TBI patients in the ICU by applying unsupervised clustering methods on data obtained from the first day post-injury.[3] These subgroups of patients had differences in composite metabolic responses, particularly related to that of lactate and glucose. However, this work did not address the more complex problem of differences in subsequent disease trajectories during the patient's ICU stay.

Previous studies have shown that clear pathophysiological patterns may emerge during the first weeks in ICU, such as different disease trajectories related to changes in Sequential Organ Failure Assessment (SOFA) score.[4] In TBI patients, variability in intracranial pressure (ICP) trajectories have been described and shown to correlate to the expression of an oedema-regulating gene, *ABCC8*.[5] Previous studies have shown that TBI is associated with extracranial complications such as acute respiratory distress syndrome (ARDS), acute kidney injury, myocardial injury, and coagulopathy.[6-8] This has led us to hypothesize that a multi-dimensional analysis of physiological, laboratory, and demographic variables during the ICU stay may describe composite longitudinal disease trajectories after TBI. A complete description must also include treatment factors, such as those described in the Therapy Intensity Level (TIL)[9] scale, which otherwise confound physiological measurements. Multidimensional factors related

to TBI disease trajectory have to date received relatively little attention, although Ghaderi *et al.* recently identified three multivariable clusters or subgroups of time series data in TBI patients exhibiting differences in physiological and haematological factors,[10] suggesting different clinical phenotypes or disease presentations, and trajectories or courses.

Therefore, the aim of this study was to identify clinical variables distinguishing disease trajectories among TBI patients admitted to the ICU. The objective is to better understand disease progression and to identify distinct trajectory-based subgroups of TBI patients, which may form the basis for future targeted therapies.

Methods

Patients

The prospective observational study, Collaborative European Neuro Trauma Effectiveness Research in TBI (CENTER-TBI, registered with ClinicalTrials.gov, number NCT02210221), enrolled 4,509 patients from 65 centres across Europe between 2014 and 2018.[11] All patients met the general inclusion criteria: clinical diagnosis of TBI, presentation at hospital within 24 hours from injury and a clinical need of a computed tomography (CT) scan. We included in this study all patients over 18 years old who were admitted to the ICU at hospital admission. Version 3.0 of the CENTER-TBI dataset was used in this study.

This study was approved by the CENTER-TBI management committee. Ethical approval was obtained for each recruiting site. The list of sites and ethical approvals details are available online.[12] Written or oral informed consent was obtained from patients or their next of kin, according to local legislation, for all patients recruited in the Core Dataset of CENTER-TBI and documented in an electronic case report form (e-CRF). In the case of oral consent, written confirmation was requested.[12]

Procedures

Data collection

Data were collected through the Quesgen e-CRF (Quesgen Systems Inc, USA), hosted on the International Neuroinformatics Coordinating Facility (INCF) platform and extracted via the INCF Neurobot tool (INCF, town, Sweden). A subset of 59 candidate admission features and daily measures, brain protein biomarkers, and interventions during the first seven days of ICU were extracted from the database; these variables covered major aspects of neurological ICU monitoring and care (Supplementary Table 1, pp 6-7). We did not extract data for pairs of features that are known to be highly covariate. CT characteristics were based on central imaging review in CENTER-TBI. The brain biomarker panel consisted of ubiquitin carboxy-terminal hydrolase L1 (UCH-L1), S100 calcium-binding protein B (S100B), Tau, neurofilament light (NFL), glial fibrillary acidic protein (GFAP) and neuron-specific enolase (NSE), as these were available in the CENTER-TBI dataset, and have shown potential in neurological evaluation and prognostication.[13,14] Blood samples were centrifuged within 60 minutes from collection, stored at -80 °C and analysed in one round using the same batch of reagents. We refer to the supplement (page 2) for further details.

Missing longitudinal data were imputed, either by interpolation set to 0 or by last observation carried forward (LOCF; Supplementary Table 2, pp 8-14). If a patient was discharged or died during the first week post-injury, all features on the following days were represented by “not available” (*NA*). Continuous features were characterised by daily means and the daily difference between maximum and minimum values if repeated measures of a feature occurred on one day.

The clustering model

Full details of the model are in the supplemental material (pp 3-5). In brief, to identify disease trajectories during the first week of ICU stay, we used a clustering method based on a mixture of probabilistic graph models to cluster patients based on baseline and longitudinal clinical features. Each graph comprised the univariate probability distributions for all features on each day and joint distributions for pairs of features that are directly correlated. Each cluster will represent a similar

disease trajectory or course. To estimate cluster membership probabilities and parameter values in the clusters, we used the iterative Expectation Maximization (EM) algorithm,[15,16] which calculates a probability for each patient's membership of each cluster and estimates cluster means and variances for continuous features and the relative frequency of categorical features.

We used an incremental clustering approach, starting with two clusters then adding one cluster at a time. This was repeated 25 times (with different seeds) until 25 models had been picked, for each cluster count from 2 to 12 (Fig 1).

To assess cluster stability, we calculated a cluster similarity index (CSI)[17] (defined as the proportion of patients with cluster assignment agreement) between all pairs of models of each number of clusters, with a higher CSI indicating more stable clustering.

To investigate the importance of each feature for the model, we calculated mutual information (MI), which is a measure of how much the distributions of the values of a feature differ between clusters.[15,18] The average MI over all 25 trajectory cluster models of each number of trajectory clusters was calculated. In addition, the average daily MI was calculated for each feature to assess the overall most important features. A qualitative analysis of the trajectories with respect to the features with highest average MI was then made.

To ascertain whether a patient's membership of a particular cluster, representing a disease trajectory, was related to late functional outcome, we analysed scores at 6 months on the Glasgow outcome scale extended (GOS-E). Scores on GOS-E range from 1 (dead) to 8 (good recovery), with an unfavourable outcome defined as a GOS-E score of 4 or less. If GOS-E was missing at 6 months but available at one or more of the other assessment timepoints (ie, 2 weeks, 3 months, and 12 months post-injury), the value was imputed centrally in CENTER-TBI.[11,19] Moreover, we evaluated the improvement in outcome predictions for mortality and unfavourable outcome beyond the International Mission for Prognosis and Clinical Trials (IMPACT) model[20] by addition of trajectory assignments using logistic regression. The improvement of predictions was evaluated by calculating Nagelkerke's R^2. The uncertainty in

predictions were estimated by bootstrap sampling with replacement 1,000 times, and the results were bias-adjusted to adjust for adding features in the model. To assess a potential site dependency of the disease trajectories, MI was calculated between site and cluster label in a post-hoc analysis. The models were created using open-source code developed in C++ by the authors and all subsequent analyses were performed using R version 4.0.5.

In a previous study, we identified six distinct clusters in the CENTER-TBI ICU stratum cohort, using only data from the first 24 h post-admission.[3] These admission clusters can be described as a composite of GCS and systemic metabolic profiles—ie, high GCS and normal metabolism (A), intermediate GCS and normal (B) or abnormal metabolism (C), low GCS and normal metabolism (D) or abnormal metabolism with either a higher incidence of intracranial pathology (E) or systemic shock (F). To investigate if the disease trajectories found in the present study could be predicted by the endotypes described at admission, probabilities of following each disease trajectory were calculated for all admission clusters.

Role of the funding source

The funding sources had no role in data collection, analysis, interpretation, writing of the manuscript, or the decision to submit for publication.

Results

2006 patients were initially eligible for the study, but 1728 patients were included in the final analysis after excluding 278 patients due to missing GOS-E at six months (Fig 2). These patients were from 54 of the 65 recruiting sites in CENTER-TBI. The median GCS score at admission was 5 (interquartile range (IQR) 3-7). 388 (22%) patients died, and 779 (45%) had unfavourable outcomes (defined as upper severe disability or worse, GOS-E ≤4). The median age was 52 years (IQR 33-67) and 1269 (73%) were male (Table 1, details in Supplementary Table 3, pp 16-22).

No distinct peak was identified when comparing the median CSI between different numbers of clusters (Supplementary Fig 1, page 27), which indicated that no particular number of clusters generated significantly more stable models, suggesting more of a continuum between the values. Six clusters (named α, β, γ, δ, ε, and ζ) were chosen to describe between-cluster differences, with numerous sensitivity analyses done (Table 2, Supplementary Fig 2, page 28) to evaluate the stability of MI of variables with an increasing number of clusters. Supplementary Fig 3 (Supplement page 29) illustrates the cluster assignments progress for increasing the number of clusters from two to twelve. The number of patients in each of the six clusters in the best model was 438 in α, 506 in β, 119 in γ, 202 in δ, 257 in ε, and 206 in ζ. Supplementary Fig 4 (Supplement page 30) and Supplementary Table 4 (Supplement page 23) shows that most patients are assigned to their final cluster with high probability.

Relations of current clustered trajectories to previously identified admission clusters[3] were explored. (Supplementary Fig 6, page 32; Supplementary Table 6, page 25). Admission cluster A (ie, patients presenting with the highest GCS and normal metabolism) had the highest probability (57%) of following a specific trajectory; the trajectory cluster associated with best outcome (α; GOS-E 7 (IQR 5-8) at 6 months). Interestingly, from admission cluster *C* with moderate TBI and affected metabolic profiles, a substantially larger proportion of patients followed the ζ trajectory associated with a 65% mortality, than admission D cluster with severe TBI and more normal metabolic profiles. In general, all other than admission cluster A are seen to have more variable relations to ICU trajectories. This suggests that clinical trajectory and course is affected by processes during the ICU period.

Generally if the clusters are ordered by outcome, from α to ζ GCS can be seen to be lower, biomarkers higher and glucose variability higher towards the clusters with worse outcome. As there was no distinct optimal number of clusters, six were chosen, as to compare movement between clusters derived from first day data and that of adding information from temporal features. We refrain therefore from further exploring characteristics of these specific six clusters and proceed with looking at descriptors

(defined as the leading variables contributing to and distinguishing clusters) of cluster models ranging from 2-12 clusters.

Glycaemic variation, brain biomarkers (Tau, UCH-L1, GFAP, S100B, NSE, and NFL), serum creatinine, and oxygen saturation had the highest overall information content, expressed by weekly average MI between cluster index and feature, in describing trajectories during the first week of ICU stay in patients with TBI (Fig 3, Table 2). A day-by-day analysis revealed these features as important on all days. In contrast, mean ICP and sodium variation showed a greater importance on early days (Supplementary Table 5, page 24). The results were consistent across models of 2 to 12 clusters. Distributions of these features on each day are presented in Supplementary Fig 5 (Supplement page 31). Thus, glucose variability and brain biomarkers were consistently the main descriptors of ICU trajectory in TBI patients.

To evaluate a potential site effect, MI of cluster membership and site was calculated in a post-hoc analysis and indicated an MI value on par with the ninth most important clustering variable.

Although the primary aim was not to identify subgroups with different outcomes, the outcomes in the different trajectory clusters differed substantially, with *α,* the most benign trajectory being associated with a 6-month mortality of 4% (*n*=16) and a 6-month unfavourable outcome of 18% (*n*=78) and the most pathological cluster (*ζ)* associated with 65% (*n*=134) mortality and 85% (*n*=174) unfavourable outcome (Fig4). 41% of patients following trajectory ζ died within 7 days post-injury, while the majority of patients following trajectory α were discharged at that timepoint. Similar patterns were seen in models of all numbers of clusters (Supplementary Fig 7, page 26). Moreover, the cluster assignments are seen to add substantial ability to discriminate both mortality and unfavourable outcome in logistic regression models including the IMPACT prediction variables (Supplementary Table 7). The addition of cluster assignments for twelve clusters was associated with the highest increase in bias-adjusted Nagelkerke's R^2, from 0·44 to 0·53 (bootstrap SE ±0·02) for mortality, and from 0·36 to 0·45 (±0·02) for

unfavourable outcome – showing that unsupervised clustering discriminates trajectories that are related to outcome.

Discussion

We have applied an unsupervised temporal clustering method to a large cohort of TBI patients treated in the ICU to investigate trajectories. The main finding is that glucose variation and biomarkers are consistently the best performing descriptors of ICU trajectories – features that have previously received relatively little attention in clinical practice. In addition, ICP mean, CSF drainage volume, creatinine, sodium variation and oxygen saturation were important descriptors of trajectories at earlier periods of the ICU stay. These findings have possible clinical implications.

The importance of glycaemic variability, rather than absolute values, has received limited investigation earlier, but has been shown to correlate with worse outcomes in general ICU cohorts and TBI ICU cohorts.[21–23] However, the mechanistic and causal relations between glycaemic variation and outcome are little understood and have not impacted treatment practices. Possible mechanistic explanations may be multifactorial representing several processes and include biological toxicity due to oxidative stress triggered by changing glucose levels, neuronal and mitochondrial damage, modulation of haemostasis, a direct association with greater sympathetic stimulation, a metabolic biomarker of injury severity, or simply a reflection of less attentive care in general.[22,23] This study suggests that glucose variation, rather than absolute values is a key variable to distinguish ICU trajectories and warrants a more extensive and targeted investigation in the future to better understand metabolic profiles, causes and effects.

Serial biomarkers have earlier been related to both outcome and secondary insults in TBI patients, but little has yet been implemented into clinical practice.[13,24–27] Our study suggests a surprisingly high

impact of biomarkers as descriptors of trajectories. Biomarkers levels can be assumed to represent ongoing processes of brain injury reflecting both neuronal or glial release (depending on biomarker) that alone or in combination[28] could reflect disease evolution, treatment effects or both. This suggests that levels and trajectories of biomarkers should also be further explored as surrogate outcome measures in TBI. Our study demonstrates that the dynamic evolution of protein biomarkers are key descriptors of trajectories and may provide an important first step towards individualised medicine in TBI care, recognizing that the predictive value of serial biomarkers needs to be evaluated in external data sets.

That sodium variation is an important descriptor of early ICU stay could be a biological effect, but probably more reflects aggressive use of hypertonic saline boluses to treat increased intracranial pressure. Harrois and colleagues have identified an association between sodium variability and mortality,[29] and rapid changes in sodium levels may induce osmotic neuronal injury. We hypothesise that as an important descriptor of ICU trajectories in TBI patients, sodium variation is more highly related to treatment intensity than biological effects.

Outcome was concealed from our clustering approach. Despite this, the identified trajectories did have a strong association with outcome. In the model of six clusters, the most benign trajectory (α) had a mortality of 4%. In comparison, the most severe trajectory (ζ) exhibited a mortality of 65%. This finding, combined with the fact that the cluster indices greatly improved outcome prediction using canonical IMPACT variables, provides evidence that disease course and clinical trajectory during the first week in ICU are independent markers of long-term outcome. The improvement in prediction of functional outcome was 25% over baseline (an increase in Nagelkerke's R^2 from 0·36-0·45 for unfavourable outcome) - critical in conceptual terms, since the events post-admission are more readily modifiable by therapy, and present more tractable targets to improve outcome.

We were unable to definitively specify an optimal number of trajectories. There is no guarantee of an optimal count of clusters. In many situations a hierarchy of clusterings can be found, where each

cluster can be further subdivided in smaller clusters, and it is subjective when to stop. Indeed, rather than the absolute number of trajectories, the most important insights provided by our study relate to the features that appeared to be of importance when describing trajectories during the first week of ICU stay in a cohort of patients with TBI.

Cluster and site shared some information, with the mutual information on par with the ninth most important cluster variable. The estimate of the mutual information is likely inflated since the covariate "site" had 54 categories. Moreover, any site effect does not exclude a generalizable biological underpinning of the cluster variables. Further explorations by site could potentially form a basis for future comparative effectiveness research and precision medicine approaches.

We must address several limitations in our manuscript. Several of the features used in the analysis had a large proportion of missing data (Supplementary Table 2, pp 8-14), as data were collected in the context of the observational study CENTER-TBI, reflecting clinical practice, and it is impossible to be certain this did not bias our results. For example, given the study's observational nature, biomarkers were more frequently sampled in patients with a more severe head injury, a subgroup with longer ICU stays. In addition, follow-up CT scans had not been systematically reported in the version of the CENTER-TBI dataset that we used and the strategy of last observation carried forward imputation may have underestimated dynamic intracranial pathologies identifiable on CT scans.

Although the aim was to describe trajectories during the first week of ICU stay, we included patients with less than seven days of stay. This might have biased the analyses as patients in this cohort with short stays in ICU (≤ 72 hours) have been shown to receive less ICP monitoring and mechanical ventilation.[30] However, as we did not feed the model with information of why a patient was discharged (dead or discharged to a ward, either as a consequence of being stable enough not needing intensive care or withdrawal of care), we believe the influence of ICU length of stay is limited. Our analysis strategy provides important information about the behaviour of patients being discharged within one week of ICU admission.

Acknowledging these limitations, the clustering method used in our study identified dynamic disease trajectories in TBI during the first week of ICU stay. Although a distinct number of clusters could not be identified, the main descriptors of TBI trajectories in this large ICU cohort were highly consistent over a range of cluster numbers. This is a clinically novel finding demonstrating that the patient course is to some extent stereotyped. Importantly, glucose variation and temporal biomarker profiles were the main clinical descriptors of ICU disease trajectories. Moreover, membership of a particular disease trajectory cluster was related to outcome which suggests biological relevance. These results suggest the need for more detailed investigation of the magnitude and mechanisms of which glucose values and variation may impact outcome in TBI. We further demonstrate the substantial discriminating power of serial biomarker measurements above clinical findings. This new result speaks to the clinical utility of *serial* biomarker measurements as part of future monitoring of TBI patients in the ICU. Indeed, the feature importance given to these suggests that consideration should be given to incorporating a panel of serial biomarkers into routine clinical practice as our work demonstrates that the clinical state is incompletely described without them. To prove clinical feasibility, the results need however to be validated in external cohorts and whether these trajectories are actionable will require prospective study. Nevertheless, these findings may be a first step to identify variables required to follow TBI trajectories in the ICU and with which to inform future targeted medicine approaches in this vulnerable patient group and complex disease.

Contributors

All authors verify that they have participated in the concept, design, analysis, writing, or revision of the manuscript and approve the final manuscript. AH, AE and DWN were responsible for the primary supervision of the project. NS, DKM, ES, DWN took part in funding acquisition. NS, ES, PS, AE, DKM, DWN took part in data collection. CÅ, AE, DWN performed data curation and accessed and verified the underlying data. CÅ performed all analyses and prepared figures and tables. SB took part in figure

preparation. AH wrote the open-source C++ code used for analysis. All authors contributed to interpretation of results and critical review and revision of the manuscript.

Declaration of interests

DKM reports grants, personal fees, and non-financial support from GlaxoSmithKline; personal fees from Neurotrauma Sciences, Lantmannen AB, Pressura, and Pfizer, outside of the submitted work. SB reports grants from Gates Cambridge foundation fellowship during the conduct of this study. PS receives parts of licensing fee for the ICM+ software from Cambridge Enterprise Ltd, UK during the conduct of this study. ES receives royalties from Springer during the conduct of this study. All other authors declare no competing interests.

Data sharing statement

CENTER-TBI encourages data sharing, and there is a data sharing statement published. Researchers can request access to the data by providing a study proposal to CENTER-TBI management committee, which can be submitted online at https://www.center-tbi.eu/data/sharing. Code as used for the statistical analysis is available at https://git.center-tbi.eu/cecilia/tbi-trajectory-clustering.

Acknowledgements

The CENTER-TBI study was supported by the European Union 7th Framework Program (EC grant 602150), with additional funding from Hannelore Kohl Stiftung (Germany), OneMind (USA) and Integra LifeSciences Corporation (USA), and NeuroTrauma Sciences (USA). The authors would like to thank all patients that have been generous to being part of CENTER-TBI. We would also like to thank all participating CENTER-TBI participants and investigators, as listed in the supplement (pp 33-42).

References

1 McCredie VA, Chavarría J, Baker AJ. How do we identify the crashing traumatic brain injury patient – the intensivist's view. *Current Opinion in Critical Care* 2021; **27**: 320–7.

2 Pugh MJ, Kennedy E, Prager EM, *et al.* Phenotyping the Spectrum of Traumatic Brain Injury: A Review and Pathway to Standardization. *J Neurotrauma* 2021; **38**: 3222–34.

3 Åkerlund CAI, Holst A, Stocchetti N, *et al.* Clustering identifies endotypes of traumatic brain injury in an intensive care cohort: a CENTER-TBI study. *Crit Care* 2022; **26**: 1–15.

4 Eriksson J, Nelson D, Holst A, Hellgren E, Friman O, Oldner A. Temporal patterns of organ dysfunction after severe trauma. *Crit Care* 2021; **25**: 165.

5 Jha RM, Elmer J, Zusman BE, *et al.* Intracranial pressure trajectories: A novel approach to informing severe traumatic brain injury phenotypes. *Critical Care Medicine* 2018; **46**: 1792–802.

6 Mascia L, Sakr Y, Pasero D, *et al.* Extracranial complications in patients with acute brain injury: a post-hoc analysis of the SOAP study. *Intensive Care Med* 2008; **34**: 720–7.

7 Robba C, Bonatti G, Pelosi P, Citerio G. Extracranial complications after traumatic brain injury: targeting the brain and the body. *Current opinion in critical care* 2020; **26**: 137–46.

8 Zygun DA, Doig CJ, Gupta AK, *et al.* Non-neurological organ dysfunction in neurocritical care. *Journal of Critical Care* 2003; **18**: 238–44.

9 Zuercher P, Groen JL, Aries MJH, *et al.* Reliability and Validity of the Therapy Intensity Level Scale: Analysis of Clinimetric Properties of a Novel Approach to Assess Management of Intracranial Pressure in Traumatic Brain Injury. *Journal of Neurotrauma* 2016; **33**: 1768–74.

10 Ghaderi H, Foreman B, Nayebi A, Tipirneni S, Reddy CK, Subbian V. A self-supervised learning-based approach to clustering multivariate time-series data with missing values (SLAC-Time):

383 An application to TBI phenotyping. *Journal of Biomedical Informatics* 2023; **143**: 104401.

384 11 Steyerberg EW, Wiegers E, Sewalt C, *et al.* Case-mix, care pathways, and outcomes in
385 patients with traumatic brain injury in CENTER-TBI: a European prospective, multicentre,
386 longitudinal, cohort study. *The Lancet Neurology* 2019; **18**: 923–34.

387 12 CENTER-TBI. CENTER-TBI Ethical Approval. https://www.center-tbi.eu/project/ethical-
388 approval.

389 13 Helmrich IRAR, Czeiter E, Amrein K, *et al.* Incremental prognostic value of acute serum
390 biomarkers for functional outcome after traumatic brain injury (CENTER-TBI): an observational
391 cohort study. *The Lancet Neurology* 2022; **21**: 792–802.

392 14 Newcombe VFJ, Ashton NJ, Posti JP, *et al.* Post-acute blood biomarkers and disease
393 progression in traumatic brain injury. *Brain* 2022; **145**: 2064–76.

394 15 Holst A. The Use of a Bayesian Neural Network Model for Classification Tasks. 1997.

395 16 Dempster AP, Laird NM, Rubin DB. Maximum Likelihood from Incomplete Data Via the
396 EM Algorithm. *Journal of the Royal Statistical Society: Series B (Methodological)* 1977; **39**: 1–22.

397 17 Lange T, Roth V, Braun ML, Buhmann JM. Stability-based validation of clustering
398 solutions. *Neural Computation* 2004; **16**: 1299–323.

399 18 Shannon CE. A Mathematical Theory of Communication. *Bell System Technical Journal*
400 1948; **27**: 379–423.

401 19 Kunzmann K, Wernisch L, Richardson S, *et al.* Imputation of Ordinal Outcomes: A
402 Comparison of Approaches in Traumatic Brain Injury. *JOURNAL OF NEUROTRAUMA* 2021; : 455–63.

403 20 Steyerberg EW, Mushkudiani N, Perel P, *et al.* Predicting Outcome after Traumatic
404 Brain Injury: Development and International Validation of Prognostic Scores Based on Admission
405 Characteristics. 2008. DOI:https://doi.org/10.1371/journal.pmed.0050165.

21 Matsushima K, Peng M, Velasco C, Schaefer E, Diaz-Arrastia R, Frankel H. Glucose variability negatively impacts long-term functional outcome in patients with traumatic brain injury. *Journal of Critical Care* 2012; **27**: 125–31.

22 Egi M, Bellomo R, Reade MC. Is reducing variability of blood glucose the real but hidden target of intensive insulin therapy? *Crit Care* 2009; **13**: 302.

23 Eslami S, Taherzadeh Z, Schultz MJ, Abu-Hanna A. Glucose variability measures and their effect on mortality: a systematic review. *Intensive Care Med* 2011; **37**: 583–93.

24 Lindblad C, Pin E, Just D, *et al.* Fluid proteomics of CSF and serum reveal important neuroinflammatory proteins in blood–brain barrier disruption and outcome prediction following severe traumatic brain injury: a prospective, observational study. *Crit Care* 2021; **25**: 1–18.

25 Shultz SR, Shah AD, Huang C, *et al.* Temporal proteomics of human cerebrospinal fluid after severe traumatic brain injury. *J Neuroinflammation* 2022; **19**: 291.

26 Thelin EP, Zeiler FA, Ercole A, *et al.* Serial Sampling of Serum Protein Biomarkers for Monitoring Human Traumatic Brain Injury Dynamics: A Systematic Review. *Front Neurol* 2017; **8**: 300.

27 Thelin EP, Nelson DW, Bellander B-M. Secondary Peaks of S100B in Serum Relate to Subsequent Radiological Pathology in Traumatic Brain Injury. *Neurocrit Care* 2014; : 217–29.

28 Thelin E, Al Nimer F, Frostell A, *et al.* A Serum Protein Biomarker Panel Improves Outcome Prediction in Human Traumatic Brain Injury. *Journal of Neurotrauma* 2019; **36**: 2850–62.

29 Harrois A, Anstey JR, van der Jagt M, *et al.* Variability in Serum Sodium Concentration and Prognostic Significance in Severe Traumatic Brain Injury: A Multicenter Observational Study. *Neurocrit Care* 2021; **34**: 899–907.

30 Huijben JA, Wiegers EJA, Lingsma HF, *et al.* Changing care pathways and between-center practice variations in intensive care for traumatic brain injury across Europe: a CENTER-TBI

analysis. *Intensive Care Medicine* 2020; **46**: 995–1004.

Figure 1: The modelling process. Models clustering two to twelve trajectories (clusters) were created separately. To converge on the best models for every number of clusters, initially, ten models of two clusters were created, with 100 patients randomly assigned to each of the two clusters from start. The trajectory cluster assignments for patients in the model with highest log likelihood (represented by a purple circle) was then used as seed to create models of three clusters – again, 100 randomly selected patients in each cluster were randomly selected from start, and in addition, 100 randomly selected patients were assigned to an incremental cluster. This optimization process was then repeated for up to twelve clusters. To assess model stability, all steps were repeated 25 times to generate 25 models of each number of clusters. Stability was assessed through cluster similarity index for each number of clusters. Importance of features was then assessed by averaging mutual information (MI) over the 25 models for each number of clusters. N_c=Number of clusters.

Figure 2: Flowchart of patient selection for the analysis. ER=Emergency room. ICU=Intensive care unit.

Figure 3: Distribution of features stratified by trajectory cluster and day. The features GCS Score, Dead and Discharged were not included in the clustering, but are illustrated here for reference. All values are normalized by $\frac{(x-\bar{x})}{sd}$. * indicates the ten features with highest mutual information.

Figure 4: Distribution of outcomes per cluster and admission patterns. A: α, the most benign trajectory, had an overall mortality of 4% (*n*=16), while ζ, the most malign trajectory, had a mortality of 65% (*n*=134). **B:** In trajectory α, most patients were discharged during the first week of ICU stay

(86% (*n*=377)). Trajectory ζ had very few patients being discharged alive during the first week, but 42% (*n*=86) died during the same period. Trajectory cluster ε had the largest proportion of patients still in ICU 7 days post-injury (70% (*n*=180)).

Research in context

Evidence before this study

The PubMed database was searched with the string “traumatic brain injury” AND (“clustering” OR “trajectory”) from database inception to July 17, 2023 to identify previous relevant studies. Several cross-sectional studies have aimed to identify patients with a traumatic brain injury who might benefit from different treatment approaches. Few studies have focused on the temporal evolution of TBI during the first days after injury. We identified 14 studies describing disease trajectories in acute traumatic brain injury. Most focused on single trajectories of intracranial pressure, biomarkers, proteomics, or neuroinflammation, and only one previous multivariate time series study assessed composite patterns. We identified one study that described pathophysiological trajectories in acute TBI in the multicenter observational TRACK-TBI cohort. Three longitudinal disease trajectories were found in this study by grouping patients according to a large number of clinical features, including baseline demographics and time-series features. These trajectories were associated with different clinical and outcome profiles. However, this study did not include brain injury biomarkers.

Added value of this study

To the best of our knowledge, our study is the first to describe pathophysiological trajectories in traumatic brain injured patients requiring intensive care in a large multicenter cohort. We identified the utility of glucose variation and a panel of brain biomarkers (ubiquitin carboxy-terminal hydrolase L1 (UCH-L1), S100 calcium-binding protein B (S100B), Tau, neurofilament light (NFL), glial fibrillary acidic protein (GFAP) and neuron-specific enolase (NSE)) as the key descriptors of disease trajectories.

Implications of all the available evidence

Multidimensional temporal patterns in disease trajectories can be identified in patients with TBI and severe trauma using physiological parameters, adding valuable information towards outcome beyond admission features alone. Although glucose levels are associated with TBI outcomes, glucose variability

has been less investigated. Glucose variation is found in our study to be the most important descriptor of ICU trajectories warranting future study on pathophysiological mechanisms and potential treatment targets. Moreover, our study, in combination with previous studies solely focusing on brain biomarker longitudinal trajectories, highlights the utility of serial brain biomarkers in TBI, suggesting incorporation of these measures in clinical care. The characterisation of disease trajectories and clinical progression of TBI could be an important step towards future targeted therapeutic approaches.

Tables

Table 1: Patient characteristics.

***N* patients**	1728
Age	52 (33, 67)
Sex	
Female	459 (27)
Male	1269 (73)
ICU Length of stay	7 (2, 16)
Total ISS	29 (25, 41)
GCS Total score at arrival	9 (4, 14)
Pupil Reactivity	
Both reacting	1403 (81)
One reacting	114 (7)
Both unreactive	211 (12)
ICP monitoring	749 (43)
Intubated	1366 (79)
Creatinine, max [μg/L]	77 (64·5, 94)
Glucose, mean first day [mmol/L]	7·7 (6·5, 9·2)
ICP, mean [mmHg]	11·7 (8·2, 15·3)
SpO_2, arrival [%]	99 (96, 100)
Sodium, mean [mmol/L]	141 (139, 144)
Rotterdam CT score	3 (3, 4)
Daily TIL, max	4 (1, 10)
GOS-E at 6 months	5 (3, 7)

1	388 (22·5)
2 or 3	268 (15·5)
4	123 (7·1)
5	241 (13·9)
6	214 (12·4)
7	229 (13·3)
8	265 (15·3)
IMPACT predicted mortality [%]	22·1 (10·7, 40·2)

Data are median (IQR) or n (%). ICU=Intensive care unit. ISS=Injury severity score. GCS=Glasgow coma scale. ICP=Intracranial pressure. SpO_2=Oxygen saturation. TIL=Therapy intensity level. GOS-E= Glasgow outcome scale extended. IMPACT= International Mission for Prognosis and Analysis of Clinical trials in TBI.

Table 2: The ten most important features describing trajectories in models of two to twelve clusters.

2	3	4	5	6	7	8	9	10	11	12
Δ Glucose	Δ Glucose	Δ Glucose	Δ Glucose	Δ Glucose	Δ Glucose	Δ Glucose	Δ Glucose	Δ Glucose	Δ Glucose	Δ Glucose
Creatinine	Creatinine	Tau	Tau	Tau	Tau	Tau	Tau	Tau	Tau	Tau
Δ SpO2	Tau	Creatinine	UCH-L1	UCH-L1	UCH-L1	UCH-L1	UCH-L1	GFAP	GFAP	GFAP
Tau	UCH-L1	UCH-L1	GFAP	GFAP	GFAP	GFAP	GFAP	UCH-L1	UCH-L1	UCH-L1
SpO_2 mean	Δ SpO_2	GFAP	Creatinine	NFL	NFL	NFL	S100B	NFL	S100B	NFL
S100B	GFAP	Δ SpO_2	NFL	S100B	Creatinine	S100B	NFL	S100B	NFL	S100B
NFL	NFL	NFL	S100B	Creatinine	S100B	Creatinine	Creatinine	Creatinine	Creatinine	Creatinine
UCH-L1	Δ pH	S100B	Δ SpO_2	Δ SpO_2	Δ SpO_2	Δ SpO_2	Δ SpO_2	Δ SpO_2	NSE	Δ SpO_2
Δ pH	S100B	NSE	NSE	NSE	NSE	NSE	NSE	NSE	Δ SpO_2	NSE
GFAP	SpO_2 mean	SpO_2 mean	SpO_2 mean	SpO_2 mean	SpO_2 mean	SpO_2 mean	SpO_2 mean	SpO_2 mean	Lactate	Lactate

Feature importance was assessed with mutual information (MI). Features or descriptors of trajectories are ranked in falling order of MI values. The top ten features are shown for models ranging from two to twelve clusters. Glycemic variation, the brain biomarkers Tau, UCH-L1, GFAP, S100B, NSE and NFL, creatinine and oxygen saturation are seen to have the highest overall average information content in describing trajectories during the first week of ICU stay in patients with TBI. The main parameters were largely consistent for models of two to twelve clusters and can be seen to additionally stabilize with an increasing number of clusters with creatinine and oxygen saturation losing importance with an increasing number of clusters. SpO_2=Oxygen saturation. NFL=Neurofilament light. NSE=Neuron-specific enolase. S100B=S100 calcium-binding protein B. GFAP=Glial fibrillary acidic protein. UCH-L1=Ubiquitin carboxy-terminal hydrolase L1.

N_C=2

N_C=3

N_C=4

...

N_C=12

x 25

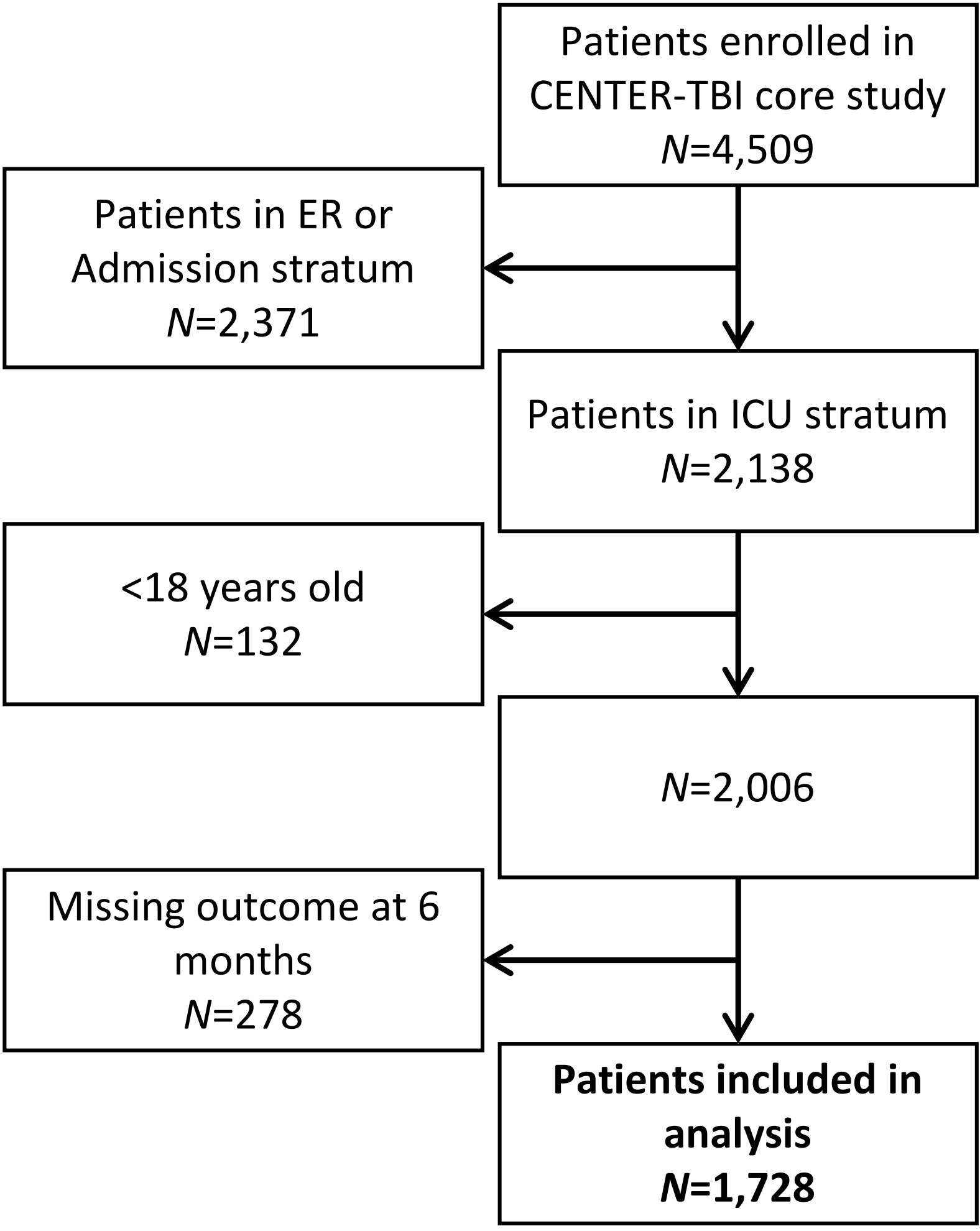
Patients enrolled in CENTER-TBI core study
N=4,509
Patients in ER or Admission stratum
N=2,371
Patients in ICU stratum
N=2,138
<18 years old
N=132
N=2,006
Missing outcome at 6 months
N=278
Patients included in analysis
***N*=1,728**

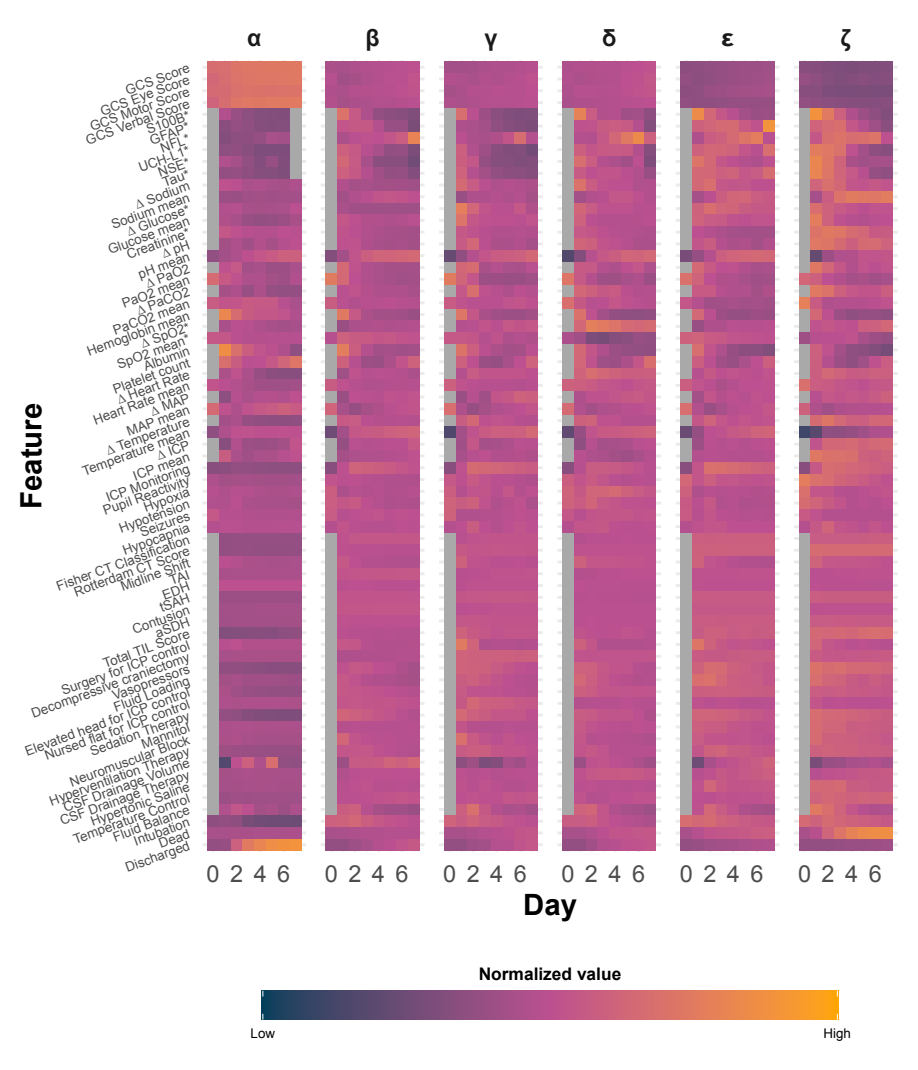
α
β
γ
δ
ε
ζ
Feature
GCS GCS Score
GCS Eye Score
GCS Motor Score
GCS Verbal Score
S100B*
GFAP*
NFL*
UCH-L1*
NSE*
Tau*
Δ Sodium
Sodium mean
Δ Glucose
Glucose mean*
Creatinine*
Δ pH
pH mean
Δ PaO2
PaO2 mean
Δ PaCO2
PaCO2 mean
Hemoglobin mean
Δ SpO2
SpO2 mean*
Albumin
Platelet count
Δ Heart Rate
Heart Rate mean
Δ MAP
MAP mean
Δ Temperature
Temperature mean
Δ ICP
ICP mean
ICP Monitoring
Pupil Reactivity
Hypoxia
Hypotension
Seizures
Hypocapnia
Fisher CT Classification
Rotterdam CT Score
Midline Shift
TAI
EDH
tSAH
Contusion
aSDH
Total TIL Score
Surgery for ICP control
Decompressive craniectomy
Vasopressors
Fluid Loading
Elevated head for ICP control
Nursed flat for ICP control
Sedation
Mannitol
Neuromuscular Block
Hyperventilation Therapy
CSF Drainage Volume
CSF Drainage Therapy
Hypertonic Saline
Temperature Control
Fluid Balance
Intubation
Dead
Discharged
0 2 4 6
Day
Normalized value
Low
High

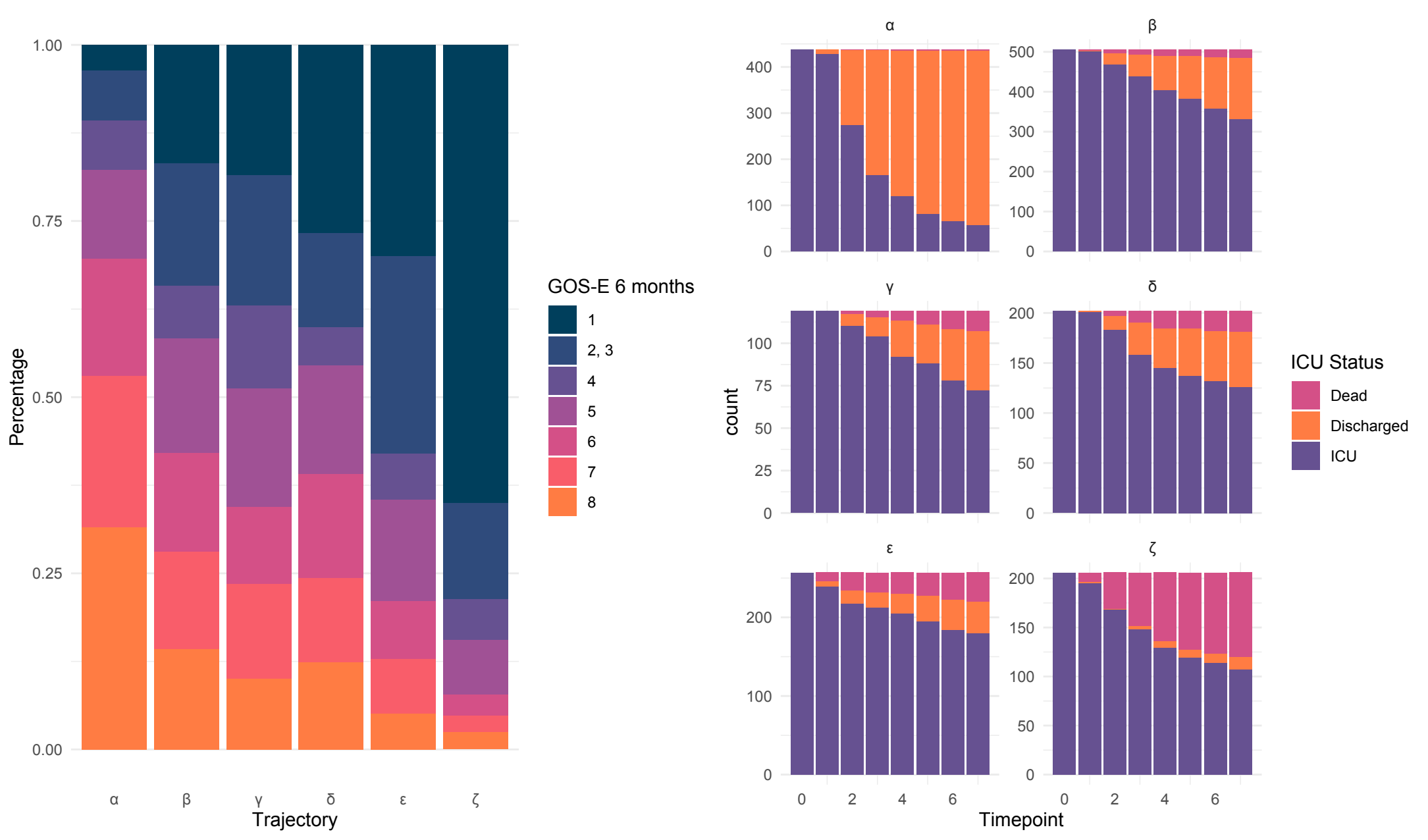
1.00
0.75
0.50
0.25
0.00
Percentage
α
β
γ
δ
ε
ζ
Trajectory
GOS-E 6 months
1
2, 3
4
5
6
7
8
α
β
γ
δ
ε
ζ
count
0
2
4
6
Timepoint
ICU Status
Dead
Discharged
ICU

Supplementary Material

Technological details of biomarker analysis 2
The clustering model 3
Supplementary Tables 6
Supplementary Figures 27
The CENTER-TBI participants and investigators 33

Technological details of biomarker analysis

The biomarker analysis is described in detail in Czeiter E, Amrein K, Gravesteijn BY, *et al.* Blood biomarkers on admission in acute traumatic brain injury: Relations to severity, CT findings and care path in the CENTER-TBI study. *EBioMedicine* 2020; **56**: 1-11.

Blood samples were centrifuged within 60 minutes from collection and stored at -80 °C. S100B and NSE were measured using an electrochemiluminescence immunoassay kit (ECLIA) (Elecsys S100 and Elecsys NSE assays) on the e 602 module of Cobas 8000 modular analyzer (Roche Diagnostics, Mannheim, Germany) at the University of Pecs (Hungary). UCH-L1, GFAP, tau, and NFL were measured with an ultrasensitive immunoassay (Single Molecule Arrays, SiMoA) at the University of Florida (USA). To avoid repeated thawing, separate aliquots were sent to the different sites, and all analyses were performed in one round of experiments using the same batch of reagents.

The clustering model

To cluster high-dimensional, longitudinal and heterogeneous data such as in this study is complex and provides substantial computational challenges. In this study we have used a mixture of probabilistic graph models,[1,2] which is well suited for this. In addition, it can handle both continuous and discrete features. Furthermore, by representing the longitudinal features as Markov chains, only dependencies between consecutive days need to be considered, significantly reducing complexity.

Each graph comprised the univariate probability distributions for all features on each day. Compensating factors (involving the joint distributions) were introduced for pairs of features on admission day with a correlation coefficient > 0·4 (i.e., age together with ASA-PS class pre-injury, age together with anticoagulant or anti-platelet treatment, and base excess together with pH) as well as compensating factors for longitudinal features on consecutive days.

In a mixture model, the complete distribution over the observed features $\boldsymbol{X}$ is written as a weighted sum of component distributions, here interpreted as clusters:

$$P(\boldsymbol{X}) = \sum_j \pi_j P(\boldsymbol{X}|c_j) \quad (1)$$

where c_j indicates that the cluster index is j and π_j is the probability of a sample to belong to that cluster. Each cluster distribution is in turn modelled as a probabilistic graph. In a probabilistic graph model it is assumed that statistical dependencies between features can be described as an acyclic graph. Then the joint distribution over $\boldsymbol{X}$ can be expressed as a product of powers of distributions over subsets of the features. More specifically, if L is the set of pairs of features (i', i) in the acyclic graph, the joint probability of cluster c_j is expressed as:

$$P(\boldsymbol{X}|c_j) = \prod_i P(x_i|c_j) \prod_{(i',i'')\in L} \frac{P(x_{i'}, x_{i''}|c_j)}{P(x_{i'}|c_j)P(x_{i''}|c_j)} \quad (2)$$

A special case of this is when there is a (first order) Markov dependence between features, such that each feature is only directly dependent on the previous feature in an ordered sequence of features $\boldsymbol{Z}_i = \{z_{i,1}, \ldots, z_{i,T}\}$:

$$P(\boldsymbol{Z}_i|c_j) = P(z_{i,1}|c_j) \prod_{t=2}^{T} P(z_{i,t}|z_{i,t-1}, c_j) = \frac{\prod_{t=2}^{T} P(z_{i,t-1}, z_{i,t}|, c_j)}{\prod_{t=2}^{T-1} P(z_{i,t}|c_j)} \quad (3)$$

The reason for using a graph model, instead of using the joint distribution over all features (such as e.g. a multivariate Gaussian distribution), is that it dramatically reduces the number of free parameters, which is critical for clustering stability. Furthermore, to avoid clusters tending to zero probability or zero variance (which is otherwise a common problem in statistical clustering), a Bayesian approach was used: The distribution over the full dataset was used as a prior when estimating the distributions in each separate cluster.

Finding the optimal number of clusters

Reliably finding clusters in high dimensional data is a challenging task. In this study, we used the expectation maximization (EM) algorithm[1,3] to estimate cluster membership probabilities and cluster parameters. One risk with the EM algorithm is that of getting stuck in local optima. One way to solve this is to run the algorithm several times from random starting points, picking the result which fits the data the best (as defined by the highest log-likelihood). How many models to create in this way is a tradeoff between computational time and optimality requirement.

To find a suitable count of clusters, we used a cluster stability approach (Fig 1). Ten models of two clusters were created with random starting points. The starting points were acquired by randomly assigning a certain number (here 100) of patients to each cluster. EM will then iteratively reshuffle the patients between the clusters to try to find a better fit. After running EM, the model with the best log likelihood out of the ten models was picked. In the next iteration, this selected model was used as a starting point for creating ten new models, each with a third cluster added and initialized by randomly assigning patients to it. Again, after running EM the best of these ten models was picked. This procedure was repeated, successively adding clusters up till 12 clusters per model. To be able to assess cluster stability, this entire procedure was repeated 25 times, yielding 25 picked models of each cluster count from 2 to 12.

We then calculated the median cluster similarity index[4] (CSI) for each number of clusters (defined as the proportion of patients with cluster assignment agreement, with a higher CSI indicating more stable clustering), and a penalty of $1/n$ was subtracted to adjust for the higher CSI naturally expected with fewer clusters. The optimal number of clusters was sought based on attempting to maximise CSI as well as clinical feasibility and sufficient cluster membership numbers.

Feature selection

To determine the importance of features included in the model, mutual information (MI)[1,5] was calculated between values of each feature and trajectory cluster label. MI is a measure of how much the distributions of the values of a feature differ between the clusters, and is defined as the difference between entropy (H) of a variable (trajectory cluster label, X) and the conditional entropy of the same variable given another feature (clinical variable, Y),

$$I(X;Y) = H(X) - HX|Y) \quad (4)$$

A higher number indicates better discrimination between the clusters.

References

1 Holst A. The Use of a Bayesian Neural Network Model for Classification Tasks. 1997.

2 Åkerlund CAI, Holst A, Stocchetti N, *et al.* Clustering identifies endotypes of traumatic brain injury in an intensive care cohort: a CENTER-TBI study. *Crit Care* 2022; **26**: 1–15.

3 Dempster AP, Laird NM, Rubin DB. Maximum Likelihood from Incomplete Data Via the EM Algorithm. *Journal of the Royal Statistical Society: Series B (Methodological)* 1977; **39**: 1–22.

4 Lange T, Roth V, Braun ML, Buhmann JM. Stability-based validation of clustering solutions. *Neural Computation* 2004; **16**: 1299–323.

5 Shannon CE. A Mathematical Theory of Communication. *Bell System Technical Journal* 1948; **27**: 379–423.

Supplementary Tables

Supplementary Table 1: Features included in the model.

Pre-injury features	***Injury characteristics***	***Lab***
Age*	Type of injury	Lactate***
Sex	Cause of injury	Base excess***
ASA-PS class pre-injury		PaO_2**
Anticoagulants or antiplatelet treatment pre-injury	***Monitoring and treatments***	SpO_2**
BMI***	ICP monitoring	$PaCO_2$**
	Intubation	pH**
Clinical presentation	Fluid balance	Albumin
GCS Eye score	Head elevation for ICP control	Sodium**
GCS Motor score*	Nursed flat for CPP management	Glucose**
GCS Verbal score	Sedation Therapy	Platelet count
Pupillary reactivity*	Neuromuscular block for ICP management	Creatinine
Heart rate**	Fluid loading for ICP management	Haemoglobin
MAP**	Vasopressors	S100B
ICP**	Hyperventilation therapy for ICP management	NSE
Body temperature**	Mannitol bolus	GFAP
	Hypertonic saline bolus	UCH-L1
CT characteristics	Temperature control for ICP management	Tau
TAI	Surgery for ICP management	NFL
EDH	Decompressive craniectomy	
aSDH	CSF drainage volume	

Contusion	***Secondary insults***	
Rotterdam CT Score	Seizures	
Fisher CT classification	Episode of hypocapnia	
	Episode of hypotension	
	Episode of hypoxia	

ASA-PS=American society of anesthesiologists' physical status classification. BMI=Body Mass Index GCS=Glasgow Coma Scale. MAP=Mean arterial pressure. ICP=Intracranial pressure. TAI=Traumatic Axonal Injury. EDH=Epidural hematoma. aSDH=Acute subdural hematoma. CT=Computed tomography. CPP=Cerebral perfusion pressure. CSF=Cerebrospinal fluid. PaO_2=Arterial partial pressure of oxygen. SpO_2=Oxygen saturation. $PaCO_2$=Arterial partial pressure of carbon dioxide. S100B=S100 calcium-binding protein B. NSE=Neuron-specific endolase. GFAP=Glial fibrillary acidic protein. UCH-L1=Ubiquitin carboxy-terminal hydrolase L1. NFL=Neurofilament light. *Feature included in the IMPACT core model, ** Daily mean and difference between daily max and min was included in the model, *** Only available at hospital admission.

Supplementary Table 2: Description of features.

Feature	Description	Unit	Imputation	Type	Data available (before imputation)								Data available (after imputation)							
					0	1	2	3	4	5	6	7	0	1	2	3	4	5	6	7
Timepoint	Day post injury (difftime("1969-12-31",Date)																			
Patients in ICU	Number of patients still in ICU				1728	1683	1419	1224	1093	1001	930	873								
gupi	ID				1728	1683	1419	1224	1093	1001	930	873	1728	1683	1419	1224	1093	1001	930	873
Discharged	set to 1 on disch date and later. Set to 0 if discharge date > timepoint or is.na(discharge date)			*discr*	1728	1683	1419	1224	1093	1001	930	873	1728	1683	1419	1224	1093	1001	930	873
Dead	set to 1 on death date and later. Set to 0 if death date > timepoint or is.na(death.date)			*discr*	1728	1683	1419	1224	1093	1001	930	873	1728	1683	1419	1224	1093	1001	930	873
Intub	set to 1 on intubated days. On TP=0, set to 1 if EDAirways=5 or 6 (intubated or mechanical ventilation)			*discr*	1728	1683	1419	1224	1093	1001	930	873	1728	1683	1419	1224	1093	1001	930	873
ICPMonitor	0=No, 1=Ventricular, 2=Ventricular+Parenchymal, 3=Parenchymal, 99=Unknown. See below table for explanation of classification of other.			*discr*	1728	1683	1419	1224	1093	1001	930	873	1728	1683	1419	1224	1093	1001	930	873
ICPMonitorYes	0=No. 1=ICPMonitorType>1.			*discr*	1728	1683	1419	1224	1093	1001	930	873	1728	1683	1419	1224	1093	1001	930	873
GCSEyes	If prehosp, "Best"		LCF	*cont*	1304	894	1180	1025	896	827	778	728	1304	1475	1372	1191	1066	979	910	855
GCSMotor	If prehosp, derived variable		LCF	*cont*	1685	840	1096	941	817	755	715	683	1685	1654	1399	1207	1076	985	915	859
GCSVerbal	If prehosp, "Best"		LCF	*cont*	1300	573	677	559	469	419	379	345	1300	1412	1272	1096	979	903	839	790
GCSScore			LCF		1636	567	671	555	463	413	372	345	1636	1608	1359	1169	1039	954	886	835
PupilResponse	Derived. Best score: 0=both reacting, 1=One unreacting, 2=both unreacting		NA0	*discr*	1633	984	1293	1127	990	919	849	784	1728	1683	1419	1224	1093	1001	930	873
Seizures	Derived. 0=No. 1=Any type of seizure		NA0	*discr*	1648	994	1295	1131	1002	922	863	801	1728	1683	1419	1224	1093	1001	930	873
Hypocapnia	Derived. 0=No. 1=Single or multiple episodes of hypocapnia		NA0	*discr*	0	972	1295	1135	1010	923	866	804	1728	1683	1419	1224	1093	1001	930	873

Feature	Description	Unit	Imputation	Type	Data available (before imputation)									Data available (after imputation)							
Timepoint					0	1	2	3	4	5	6	7		0	1	2	3	4	5	6	7
Hypotension	Derived. 0=No. 1=Single or multiple episodes of hypotension		NA0	*discr*	1707	1007	1311	1155	1025	938	878	819		1728	1683	1419	1224	1093	1001	930	873
Hypoxia	Derived. 0=No. 1=Single or multiple episodes of hypoxia		NA0		1707	1007	1311	1155	1025	938	878	819		1728	1683	1419	1224	1093	1001	930	873
HRMax	Vitals CRF. First HR for TP=0	min^{-1}		*cont*																	
HRMin	Vitals CRF.	min^{-1}		*cont*																	
HRDiff	Calculated: HRMax-HRMin	min^{-1}	interpol	*cont*	0	1048	1369	1190	1055	973	905	848		0	1048	1377	1204	1072	982	912	848
HRMean		min^{-1}	interpol	*cont*	1560	1048	1369	1190	1055	973	905	848		1560	1592	1396	1204	1072	982	912	848
MAPMax	Max calculated MAP from Vitals and HV. SBP set to NA if outside range 300-30, DBP <10. (SBP+2*DBP)/3	mmHg		*cont*																	
MAPMin	Min calculated MAP from Vitals and HV	mmHg		*cont*																	
MAPMean	Mean of HourlyValues calculated two-hourly MAP	mmHg	interpol	*cont*	1577	1065	1371	1191	1059	974	909	847		1577	1604	1393	1200	1068	979	910	847
MAPDiff		mmHg	interpol	*cont*	0	570	944	858	750	697	635	579		0	570	955	870	773	712	645	579
ICPMax	HourlyValues CRF. One patient with comment "EVD, ICP in mmH2O", the recorded ICP values were divided by 1.3595 (cmH2O -> mmHg). Set to NA if outside range -10 - 140.	mmHg		*cont*																	
ICPMin	HourlyValues CRF. One patient with comment "EVD, ICP in mmH2O", the recorded ICP values were divided by 1.3595 (cmH2O -> mmHg). Set to NA if outside range -10 - 140.	mmHg		*cont*																	
ICPMean	Mean of HourlyValues calculated two-hourly ICP. One patient with comment "EVD, ICP in mmH2O", the recorded ICP values were divided by 1.3595 (cmH2O -> mmHg). Set to NA if outside range -10 - 140.	mmHg	interpol	*cont*	0	347	681	658	591	542	488	427		0	347	686	668	608	554	491	427

Feature	Description	Unit	Imputation	Type	Data available (before imputation)									Data available (after imputation)							
Timepoint					0	1	2	3	4	5	6	7		0	1	2	3	4	5	6	7
ICPDiff	ICPMax-ICPMin each day.	mmHg	interpol	*cont*	0	347	681	658	591	542	488	427		0	347	686	668	608	554	491	427
TempMax	First temp for TP=0	°C		*cont*																	
TempMin		°C		*cont*																	
TempMean	Calculated if >1 temperature value each day	°C	interpol	*cont*	818	970	1357	1179	1049	970	902	841		818	1286	1383	1203	1070	981	910	841
TempDiff	Calculated: TempMax-TempMin	°C	interpol	*cont*	0	970	1357	1179	1049	970	902	841		0	970	1368	1202	1070	981	910	841
PaO_2Max		kPa		*cont*																	
PaO_2Min	First PaO2 for TP=0	kPa		*cont*																	
PaO_2Mean	If PaO2Mean>55, divided by 7.5 (conversion from mmHg to kPa). If >100, set to NA	kPa	interpol	*cont*	967	799	1207	1014	909	838	790	733		969	1196	1241	1069	958	881	815	733
PaO_2Diff	Calculated: PaO_2Max-PaO_2Min	kPa	interpol		0	799	1207	1014	909	838	790	733		0	799	1220	1067	958	880	814	733
SpO_2Max		%		*cont*																	
SpO_2Min	First SpO2 for TP=0	%		*cont*																	
SpO_2Mean	If SpO2<50, set to NA.	%	interpol		1510	1039	1368	1186	1051	967	900	844		1510	1577	1393	1203	1070	979	910	844
SpO_2Diff	Calculated: SpO_2Max-SpO_2Min	%	interpol		0	1039	1368	1186	1051	967	900	844		0	1039	1376	1203	1070	979	910	844
$PaCO_2$Max	First $PaCO_2$ for TP=0	kPa		*cont*																	
$PaCO_2$Min		kPa		*cont*																	
$PaCO_2$Mean	If $PaCO_2$Mean >15, divided by 7.5 (conversion from mmHg to kPa). If >30, set to NA.	kPa	interpol	*cont*	969	799	1207	1016	910	841	790	733		969	1196	1244	1071	957	880	814	733
$PaCO_2$Diff	Calculated: $PaCO_2$Max-$PaCO_2$Min	kPa	interpol		0	799	1207	1016	910	841	790	733		0	799	1221	1067	957	880	814	733
pHMax	First pH for TP=0. Set to NA if <6			*cont*																	
pHMin				*cont*																	
pHMean			interpol		969	803	1207	1013	908	839	792	733		967	1194	1242	1070	958	880	814	733
pHDiff			interpol		0	803	1207	1013	908	839	792	733		0	803	1219	1066	958	881	815	733
AlbuminMin		g/L		*cont*																	

Feature	Description	Unit	Imputation	Type	Data available (before imputation)									Data available (after imputation)							
Timepoint					0	1	2	3	4	5	6	7		0	1	2	3	4	5	6	7
AlbuminMean	Set to NA if >100.	g/L	interpol	*cont*	0	643	744	626	529	469	390	286		0	643	807	716	617	533	421	286
SodiumMax	First sodium for TP=0. Set to NA if >185.	mmol/L		*cont*																	
SodiumMin		mmol/L		*cont*																	
SodiumMean	Calculated if >1 sodium value one day	mmol/L	interpol	*cont*	0	1304	1273	1070	936	857	700	525		0	1304	1317	1118	987	892	717	525
SodiumDiff	Calculated: SodiumMax-SodiumMin	mmol/L	interpol	*cont*	0	1304	1273	1070	936	857	700	525		0	1304	1317	1118	987	892	717	525
GlucoseMax	First glucose for TP=0	mmol/L		*cont*																	
GlucoseMin		mmol/L		*cont*																	
GlucoseMean	Calculated if >1 glucose value one day		interpol	*cont*	0	1249	1164	952	824	758	623	465		0	1249	1234	1027	900	812	644	465
GlucoseDiff	Calculated: GlucoseMax-GlucoseMin		interpol	*cont*	0	1249	1164	952	824	758	623	465		0	1249	1234	1027	900	812	644	465
PlateletMin		$*10^{-9}$/L		*cont*																	
PlateletMean		$*10^{-9}$/L	interpol		0	1300	1284	1077	940	837	685	519		0	1300	1328	1128	985	884	706	519
CreatinineMax		µmol/L		*cont*																	
CreatinineMean	Set to NA if <10.	µmol/L	interpol	*cont*	0	1299	1259	1054	919	823	687	511		0	1299	1314	1123	985	880	706	511
HbMin	Hb first for TP=0. Set to NA if outside range 20-210.	g/L		*cont*																	
HbMean		g/L	interpol	*cont*	0	1322	1306	1092	955	860	703	529		0	1322	1339	1137	991	898	719	529
TAI	From central review. Derived: If missing, imputed by last value carried forward.		LCF	*discr*	0	1340	142	19	13	4	3	2		0	1340	1246	1071	957	876	813	759
EDH	From central review. Derived: If missing, imputed by last value carried forward.		LCF	*discr*	0	1338	142	19	13	4	3	2		0	1338	1245	1071	957	876	813	759
aSDH	From central review. Derived: If missing, imputed by last value carried forward.		LCF	*discr*	0	1337	141	19	13	4	3	2		0	1337	1242	1070	957	876	813	759
Contusion	From central review. Derived: If missing, imputed by last value carried forward.		LCF	*discr*	0	1339	141	19	13	4	3	2		0	1339	1245	1070	956	875	812	758

Feature	Description	Unit	Imputation	Type	Data available (before imputation)									Data available (after imputation)							
Timepoint					0	1	2	3	4	5	6	7		0	1	2	3	4	5	6	7
tSAH	From central review. Derived: If missing, imputed by last value carried forward.		LCF	*discr*	0	1336	142	19	13	4	3	2		0	1336	1242	1067	953	873	810	757
RotterdamCTScore	From central review		LCF	*discr*	0	1353	431	64	29	20	17	9		0	1353	1276	1098	981	897	833	780
MidlineShiftmm	From central review. If >30 mm, set to NA.	mm	NA0	*cont*	0	402	225	52	43	26	27	23		1728	1683	1419	1224	1093	1001	930	873
MidlineShift	1=Yes, 0=No			discr	0	402	225	52	43	26	27	23		0	402	440	397	369	340	321	304
FisherClassification	From central review		LCF	*discr*	0	1352	431	64	29	20	17	9		0	1352	1275	1097	980	896	832	779
TotalTIL	Total Therapy Intensity Level Score			*cont*	0	797	1157	1002	897	822	758	710		0	797	1157	1002	897	822	758	710
Position	Head elevation for ICP control		LCF	*discr*	0	797	1157	1004	898	822	758	710		0	797	1193	1076	975	900	842	793
PositionNursedFlat	Nursed flat for CPP management		LCF	*discr*	0	795	1154	1002	896	820	756	708		0	795	1190	1074	973	898	840	791
SedationTherapy	Derived. '0=No, 1=Low dose required for mechanical ventilation, 2=Higher dose sedation for ICP control (not aiming for burst suppression), 3=Metabolic suppression for ICP control w high dose barbiturates or propofol		LCF	*discr*	0	796	1157	1002	896	821	757	710		0	796	1193	1076	975	900	842	793
NeuromuscBlock	Neuromuscular block. 0=No, 1=Yes.		LCF	*discr*	0	797	1157	1004	897	821	758	710		0	797	1193	1076	975	900	842	793
CSFDrainageTherapy	0=No, 1=<120 ml/day, 2= >=120 ml/day			*discr*	0	793	1154	1001	895	820	758	709		0	793	1191	1075	974	899	842	793
CSFDrainageVol	Set to NA if CSFDrainageTherapy==0	ml	LCF	*cont*	0	51	104	129	109	120	117	123		0	51	108	133	123	125	121	123
FluidLoading	Fluid loading for maintenance of cerebral perfusion. 0 = No, 1=Yes		LCF	*discr*	0	797	1156	1003	896	821	758	710		0	797	1192	1075	974	899	841	792
Vasopressor	Vasopressor therapy required for management of cerebral perfusion		LCF	*discr*	0	797	1157	1003	896	821	758	709		0	797	1193	1076	975	900	842	793
HyperventTherapy	Derived. For ICP control: 0=No, 1=PaCO2 4.6-5.3 kPa for ICP control, 2=PaCO2 4.0-4.5 kPa for ICP control, 3=PaCO2<4 kPa for ICP control		LCF	*discr*	0	797	1156	1002	895	820	757	709		0	797	1192	1075	974	899	841	792

Feature	Description	Unit	Imputation	Type	Data available (before imputation)									Data available (after imputation)							
Timepoint					0	1	2	3	4	5	6	7		0	1	2	3	4	5	6	7
Mannitol	Derived. 0=No, 1=Mannitol < 2g/kg/24h, 2=Mannitol >2g/kg/24h		LCF	*discr*	0	797	1157	1003	896	821	758	710		0	797	1193	1076	975	900	842	793
Saline	Derived. 0=No, 1=Hypertonic saline <0.3g/kg/24h, 2=Hypertonic saline >0.3g/kg/24h		LCF	*discr*	0	797	1157	1002	896	821	758	710		0	797	1193	1076	975	900	842	793
Tempcontrol	Derived. 0=No, 1=Treatment of temp >38C or spont temp <34.5, 2=Mild hypothermia for ICP control (>35C), 3=Hypothermia <35C		LCF	*discr*	0	797	1157	1003	897	821	758	710		0	797	1193	1076	975	900	842	793
ICPSurgery	Intracranial surgery for progressive mass lesion, not scheduled on admission		LCF	*discr*	0	797	1157	1003	897	822	758	710		0	797	1193	1076	975	900	842	793
DecomprCran	Decompressive craniectomy extracted from surgeries CRF.		LCF	*discr*	0	798	1157	1006	899	823	759	710		0	798	1194	1077	976	901	843	794
FluidBal	FluidIn-(FluidOutUrine + FluidOutGastric + FluidOutCSFDrain + FluidOutOther). Set to NA if out of range -10000 - 15000		interpol	*discr*	0	728	1111	973	869	806	741	691		0	728	1133	1019	909	840	771	691
S100B		µg/L	interpol	*cont*	0	522	1062	646	300	253	151	22		0	522	1098	677	311	262	151	22
NSE		ng/mL	interpol	*cont*	0	538	1068	653	298	251	150	22		0	538	1102	682	309	262	150	22
GFAP		ng/mL	interpol	*cont*	0	561	1019	596	280	240	128	4		0	561	1056	632	295	247	130	4
UCH-L1		pg/mL	interpol	*cont*	0	542	1037	604	278	234	127	4		0	542	1074	640	293	241	129	4
Tau		pg/mL	interpol	*cont*	0	542	1032	619	284	235	127	4		0	542	1070	649	297	245	129	4
NFL		pg/mL	interpol	*cont*	0	564	1068	623	281	232	119	4		0	564	1103	655	295	240	121	4
Age				*cont*	1728	0	0	0	0	0	0	0		1728	0	0	0	0	0	0	0
Sex	1=Male, 2=Female			*cont*	1728	0	0	0	0	0	0	0		1728	0	0	0	0	0	0	0
ASAClass				*discr*	1650	0	0	0	0	0	0	0		1650	0	0	0	0	0	0	0

Feature	Description	Unit	Imputation	Type	Data available (before imputation)									Data available (after imputation)							
Timepoint					0	1	2	3	4	5	6	7		0	1	2	3	4	5	6	7
InjType	1=Closed, 2=Blast, 3=Crush, 5=Penetrating, 6=Penetrating-perforating, 7=Penetrating-tangential, 8=Closed with open depressed skull fracture			*discr*	1698	0	0	0	0	0	0	0		1698	0	0	0	0	0	0	0
InjCause	1=Road traffic incident, 2=Incidental fall, 3=Other non-intentional injury, 4=Violence/assault, 5=Act of mass violence, 6=Suicide attempt			*discr*	1601	0	0	0	0	0	0	0		1601	0	0	0	0	0	0	0
GOSE6mo	Imputed score			*discr*	1728	0	0	0	0	0	0	0		1728	0	0	0	0	0	0	0
HeadISS				*discr*	1728	0	0	0	0	0	0	0		1728	0	0	0	0	0	0	0
ExtracranISSHighest				*discr*	1728	0	0	0	0	0	0	0		1728	0	0	0	0	0	0	0
TotalISS				*discr*	1695	0	0	0	0	0	0	0		1695	0	0	0	0	0	0	0
Lactate	At arrival. Not available inhospital	mmol/L		*cont*	826	0	0	0	0	0	0	0		826	0	0	0	0	0	0	0
Anticoags	At arrival			*discr*	1626	0	0	0	0	0	0	0		1626	0	0	0	0	0	0	0
BE	At arrival. Not available inhospital			*cont*	905	0	0	0	0	0	0	0		905	0	0	0	0	0	0	0
BMI	At arrival	kg/m^2		*cont*	1210	0	0	0	0	0	0	0		1210	0	0	0	0	0	0	0

All features extracted from the CENTER-TBI dataset. In case of imputation, the method is described. Data on missingness is also provided in the table. *=Not included in analyses. ICU=Intensive care unit, ICP=Intracranial pressure, GCS=Glasgow Coma Scale, HR=Heart Rate, MAP=Mean arterial pressure,PaO_2=Arterial partial pressure of oxygen, SpO_2=Oxygen saturation, $PaCO_2$=Arterial partial pressure of carbon dioxide, Hb=Hemoglobin, TAI=Traumatic axonal injury, EDH=Epidural hematoma, aSDH=acute subdural hematoma, tSAH=traumatic subarachnoid hemorrhage, CT=Computed tomography, CSF=Cerebrospinal fluid, S100B=S100 calcium-binding protein B, NSE=Neuron-specific endolase, GFAP=Glial fibrillary atrial protein, UCH-L1=Ubiquitine carboxy-terminal hydrolase L1, NFL=Neurofilament light, ASAclass=American society of anaesthesiologists' physical status classification, GOSE6mo=Glasgow outcome scale extended at 6 months post-injury, ISS=Injury severity score, BE=Base excess, BMI=Body mass index, LCF=Last carried forward, NA0=Missings are imputed by 0, interpol=interpolation, discr=discrete, cont=continuous.

Supplementary Table 3: Patient characteristics of clusters.

	All patients	α	β	γ	δ	ε	ζ
N patients	1728	438	506	119	202	257	206
Age	52 (33, 67)	52 (35, 65)	50 (32, 66)	51 (32, 65)	57 (35, 68)	51 (33, 65)	53 (32, 72)
Sex							
Female	459 (27)	104 (24)	120 (24)	26 (22)	57 (28)	95 (37)	57 (28)
Male	1269 (73)	334 (76)	386 (76)	93 (78)	145 (72)	162 (63)	149 (72)
GOS-E at 6 months	5 (3, 7)	7 (5, 8)	5 (3, 7)	5 (3, 6)	5 (1, 6)	3 (1, 5)	1 (1, 3)
1	388 (22·5)	16 (3·7)	85 (16·8)	22 (18·5)	54 (26·7)	77 (30)	134 (65)
2 or 3	268 (15·5)	31 (7·1)	88 (17·4)	22 (18·5)	27 (13·4)	72 (28)	28 (13·6)
4	123 (7·1)	31 (7·1)	38 (7·5)	14 (11·8)	11 (5·4)	17 (6·6)	12 (5·8)
5	241 (13·9)	55 (12·6)	82 (16·2)	20 (16·8)	31 (15·3)	37 (14·4)	16 (7·8)
6	214 (12·4)	73 (16·7)	71 (14)	13 (10·9)	30 (14·9)	21 (8·2)	6 (2·9)
7	229 (13·3)	94 (21·5)	70 (13·8)	16 (13·4)	24 (11·9)	20 (7·8)	5 (2·4)
8	265 (15·3)	138 (31·5)	72 (14·2)	12 (10·1)	25 (12·4)	13 (5·1)	5 (2·4)
ASA-PS classification pre-injury							
1	922 (53·4)	244 (55·7)	277 (54·7)	65 (54·6)	112 (55·4)	134 (52·1)	90 (43·7)
2	545 (31·5)	137 (31·3)	163 (32·2)	38 (31·9)	53 (26·2)	87 (33·9)	67 (32·5)
3	170 (9·8)	41 (9·4)	45 (8·9)	13 (10·9)	22 (10·9)	21 (8·2)	28 (13·6)
4	13 (0·8)	5 (1·1)	2 (0·4)	*NA*	1 (0·5)	2 (0·8)	3 (1·5)
NA	78 (4·5)	11 (2·5)	19 (3·8)	3 (2·5)	14 (6·9)	13 (5·1)	18 (8·7)
Anticoagulant or anti-platelet treatment pre-injury	282 (16·3)	76 (17·4)	73 (14·4)	19 (16)	35 (17·3)	38 (14·8)	41 (19·9)

	All patients	α	β	γ	δ	ε	ζ
Type of injury							
Closed	1575 (91·1)	402 (91·8)	444 (87·7)	114 (95·8)	184 (91·1)	247 (96·1)	184 (89·3)
Blast	2 (0·1)	*NA*	*NA*	*NA*	1 (0·5)	*NA*	1 (0·5)
Crush	45 (2·6)	5 (1·1)	23 (4·5)	3 (2·5)	8 (4)	1 (0·4)	5 (2·4)
Penetrating	14 (0·8)	4 (0·9)	6 (1·2)	*NA*	3 (1·5)	*NA*	1 (0·5)
Penetrating-Perforating	8 (0·5)	2 (0·5)	1 (0·2)	1 (0·8)		3 (1·2)	1 (0·5)
Penetrating-Tangential	1 (0·1)	*NA*	*NA*	*NA*	*NA*	*NA*	1 (0·5)
Closed with open depressed skull fracture	53 (3·1)	13 (3)	20 (4)	1 (0·8)	3 (1·5)	5 (1·9)	11 (5·3)
NA	30 (1·7)	12 (2·7)	12 (2·4)	*NA*	3 (1·5)	1 (0·4)	2 (1)
Cause of injury	7						
Road traffic collission	745 (43·1)	163 (37·2)	221 (43·7)	52 (43·7)	90 (44·6)	133 (51·8)	86 (41·7)
Incidental fall	700 (40·5)	199 (45·4)	207 (40·9)	46 (38·7)	77 (38·1)	89 (34·6)	82 (39·8)
Other non-intentional injury	58 (3·4)	14 (3·2)	20 (4)	6 (5)	6 (3)	10 (3·9)	2 (1)
Violence/Assault	61 (3·5)	22 (5)	12 (2·4)	5 (4·2)	7 (3·5)	7 (2·7)	8 (3·9)
Act of mass violence	1 (0·1)	1 (0·2)					9 (4·4)
Suicide attempt	36 (2·1)	7 (1·6)	9 (1·8)	1 (0·8)	5 (2·5)	5 (1·9)	19 (9·2)
NA	127 (7·3)	32 (7·3)	37 (7·3)	9 (7·6)	17 (8·4)	13 (5·1)	
Pupil Reactivity							
Both reacting	1403 (81·2)	412 (94·1)	432 (85·4)	100 (84)	154 (76·2)	186 (72·4)	119 (57·8)
One reacting	114 (6·6)	19 (4·3)	28 (5·5)	4 (3·4)	24 (11·9)	20 (7·8)	19 (9·2)
Both unreactive	211 (12·2)	7 (1·6)	46 (9·1)	15 (12·6)	24 (11·9)	51 (19·8)	68 (33)
	2						
Extracranial ISS, highest	9 (0, 16)	4 (0, 9)	9 (0, 16)	9 (0, 16)	9 (1, 16)	9 (0, 16)	9 (0, 16)
Head ISS	25 (16, 25)	16 (9, 16)	25 (16, 25)	25 (16, 25)	25 (16, 25)	25 (25, 25)	25 (16, 25)
Total ISS	29 (25, 41)	24 (16, 29)	32 (25, 43)	32·5 (25, 43)	34 (25, 45)	34 (25, 50)	38 (25, 57)

	All patients	α	β	γ	δ	ε	ζ
ICP monitoring	749 (43·3)	27 (6·2)	261 (51·6)	73 (61·3)	91 (45)	166 (64·6)	131 (63·6)
Surgery for ICP control	145 (8·4)	10 (2·3)	38 (7·5)	17 (14·3)	16 (7·9)	39 (15·2)	25 (12·1)
Intubated	1366 (79·1)	175 (40)	462 (91·3)	105 (88·2)	170 (84·2)	253 (98·4)	201 (97·6)
GCS Total score at arrival	9 (4, 14)	14 (12, 15)	8 (3, 13)	7 (3, 13)	8 (4, 13)	6 (3, 8)	4 (3, 9)
GCS Motor score at arrival	5 (1, 6)	6 (5, 6)	5 (1, 6)	4 (1, 6)	4 (1, 6)	2 (1, 5)	1 (1, 5)
GCS Verbal score at arrival	2 (1, 4)	4 (2, 5)	2 (1, 4)	2 (1, 4)	2 (1, 4)	1 (1, 2)	1 (1, 2)
GCS Eye score at arrival	2 (1, 4)	4 (3, 4)	2 (1, 4)	2 (1, 4)	2 (1, 4)	1 (1, 3)	1 (1, 3)
Base excess	-2·9 (-5·7, -0·9)	-1·5 (-3·2, 0·2)	-2·5 (-5, 0)	-3·6 (-6, -1·9)	-3·7 (-6, -1·2)	-3·1 (-5·9, -1)	-5·5 (-10·1, -1·9)
Lactate [mmol/L]	2·2 (1·4, 3·4)	1·7 (1·2, 2·7)	2·1 (1·4, 3·3)	2·4 (1·5, 3·5)	2·4 (1·6, 4·1)	1·9 (1·2, 3)	3·4 (2, 6·8)
Body mass index [kg*m^{-2}]	24·8 (22·9, 27·7)	25·3 (22·9, 27·7)	24·8 (22·9, 27·6)	25·1 (22·9, 29·5)	24·7 (23, 27·8)	24·7 (22·2, 27·6)	24·7 (22·5, 27·7)
Creatinine [µmol/L]							
First day	75 (62, 89)	76 (64, 88)	71 (60, 87)	79 (68, 89)	76 (64, 90)	68 (57, 82)	87 (68, 105)
Max any days	77 (64·5, 94)	76 (65, 89)	75 (62·75, 89)	80·5 (66, 96·25)	78·5 (65, 97·25)	73 (61, 86)	97 (76, 131·5)
Albumin, first day [g/L]	37 (32, 41)	40 (37, 43)	38 (33, 42)	35 (32, 40)	35 (31, 38)	36 (31, 39)	35 (30, 38)
Glucose, mean first day [mmol/L]	7·7 (6·5, 9·2)	7 (6·1, 8·2)	7·5 (6·5, 8·9)	8·1 (6·9, 10·3)	7·8 (6·6, 9·7)	8·2 (7·1, 9·6)	9·1 (7·3, 10·9)
Glucose, Δ first day [mmol/L]	0 (0, 0·8)	0 (0, 0·1)	0 (0, 0)	0 (0, 2·3)	0 (0, 1·7)	0·2 (0, 2)	0 (0, 2·6)
Hemoglobin, first day [g/L]	130 (115, 142)	138 (126, 147)	131 (118, 141)	130 (111, 142)	126 (112, 139)	121 (105, 135)	121 (103, 136)
Heart rate, Δ first day [min^{-1}]	22 (12, 34)	21 (10, 32)	20 (10, 28)	22 (15, 35)	29 (16, 47)	22 (13, 34)	27 (16, 43)
Heart rate, mean day of injury [min^{-1}]	82 (71, 99)	80 (71, 91)	80 (70, 100)	85 (72, 100)	82 (70, 100)	84 (70, 100)	90 (76, 110)
Hypocapnic event, any day	76 (4·4)	3 (0·7)	17 (3·4)	6 (5)	16 (7·9)	14 (5·4)	20 (9·7)
Hypotensive event, any day	557 (32·2)	45 (10·3)	176 (34·8)	56 (47·1)	101 (50)	80 (31·1)	99 (48·1)
Hypoxic event, any day	489 (28·3)	48 (11)	122 (24·1)	47 (39·5)	104 (51·5)	75 (29·2)	93 (45·1)

	All patients	α	β	γ	δ	ε	ζ
Seizures							
day of injury	103 (5·96)	23 (5·3)	32 (6·3)	10 (8·4)	10 (5)	16 (6·2)	12 (5·8)
any day	192 (11·1)	31 (7·1)	65 (12·8)	15 (12·6)	29 (14·4)	34 (13·2)	18 (8·7)
Fluid balance [ml]							
First day	469 (-185, 1445)	120 (-374, 587)	742 (-6, 1715)	764 (-59, 1734)	743 (-223, 1756)	360 (-205, 1232)	1179 (-130, 3430)
First week	590 (0, 3525)	0 (0, 987)	721 (-442, 3930)	1839 (0, 4584)	869 (0, 3688)	1601 (0, 4846)	2036 (0, 5558)
ICP, mean [mmHg]							
First day	11 (6, 16)	15 (9, 18)	10 (6, 14)	10 (7, 14)	9 (3, 15)	10 (6, 16)	16 (11, 28)
All days	11·7 (8·2, 15·3)	10·8 (7, 13·3)	11·2 (8, 14·1)	11·5 (9, 15)	9·7 (5·9, 13·1)	11·5 (7·8, 15·4)	15·3 (12, 24·4)
Max all days	15 (11, 19)	13 (8, 17·25)	15 (11, 18)	15 (11, 17)	13 (9, 16·25)	16 (11, 19)	20 (16, 36)
ICP, Δ [mmHg]							
First day	6 (3, 12)	6 (0, 11)	6 (2, 11)	7 (3, 13)	6 (3, 9)	6 (3, 11)	8 (4, 16)
Max all days	17 (12, 24)	12 (8, 16·75)	17 (12, 24)	17 (13, 23)	15 (12, 19·25)	17 (12, 22)	26 (16, 44)
MAP, arrival [mmHg]	97 (85, 110)	97 (87, 110)	97 (85, 109)	101 (89, 112)	98 (85, 112)	100 (87, 114)	95 (79, 110)
Body temperature, arrival [°C]	36 (35·4, 36·7)	36,4 (35·9, 36·9)	36·2 (35·4, 36·7)	36 (35·3, 36·6)	36·1 (35·3, 36·7)	36 (35·2, 36·6)	35·6 (34·6, 36·3)
$PaCO_2$, arrival [kPa]	5·5 (4·8, 6·2)	5·5 (5, 6·1)	5·3 (4·7, 6·1)	5·4 (4·8, 6·3)	5·6 (4·8, 6·4)	5·4 (4·8, 6)	5·9 (5·1, 7)
PaO_2, arrival [kPa]	20·4 (11·6, 35·2)	19·1 (11·1, 31·8)	22·7 (11·6, 37·6)	20·6 (13·1, 34·7)	18·9 (12, 37·3)	19·5 (12·2, 34·1)	19·2 (10·6, 28·9)
pH, arrival	7·35 (7·28, 7·39)	7·37 (7·33, 7·4)	7·35 (7·31, 7·41)	7·32 (7·26, 7·38)	7·32 (7·24, 7·38)	7·35 (7·28, 7·39)	7·29 (7·17, 7·36)
SpO_2, arrival [%]	99 (96, 100)	98 (96, 100)	99 (96, 100)	99 (97, 100)	98 (95, 100)	99 (97, 100)	98 (95, 100)
Sodium, mean all days [mmol/L]							
Mean all days	141 (139, 144)	140 (138, 142)	142 (140, 144)	140 (138, 143)	142 (138, 144)	142 (140, 145)	144 (140, 147)
Max all days	143·5 (141, 147)	141 (139, 143)	144 (142, 147)	143 (140, 146)	144 (141, 148)	146 (142, 150)	147 (143, 153·5)
Sodium, max daily Δ [mmol/L]	0 (0, 4)	0 (0, 3)	0 (0, 0)	2 (0, 5)	3 (0, 5)	4 (1, 6)	3 (0, 7)
Platelet count, lowest [$*10^9$/L]	150 (112, 195)	190 (152, 231)	140 (109, 174)	147 (109, 172)	148 (107, 192)	142 (108, 174)	129 (96, 184)

	All patients	α	β	γ	δ	ε	ζ
CT characteristics							
Rotterdam CT score	3 (3, 4)	3 (2, 3)	3 (3, 4)	3 (3, 5)	3 (3, 4)	4 (3, 5)	4 (3, 5)
Fisher Classification	2 (2, 4)	2 (1, 2)	2 (2, 4)	2 (2, 4)	2 (2, 3)	3 (2, 4)	2 (2, 4)
Midline shift	311 (18)	31 (7·1)	82 (16·2)	27 (22·7)	45 (22·3)	79 (30·7)	47 (22·8)
Midline Shift in mm	0 (0, 0)	0 (0, 0)	0 (0, 0)	0 (0, 3·5)	0 (0, 2)	0 (0, 5)	0 (0, 4)
TAI	210 (12·2)	28 (1·6)	83 (4·8)	14 (0·8)	22 (1·3)	36 (2·1)	27 (1·6)
aSDH	640 (37)	104 (6)	197 (11·4)	50 (2·9)	80 (4·6)	116 (6·7)	93 (5·4)
Contusion	756 (43·8)	138 (8)	254 (14·7)	50 (2·9)	96 (5·6)	126 (7·3)	92 (5·3)
EDH	250 (14·5)	66 (3·8)	71 (4·1)	16 (0·9)	31 (1·8)	37 (2·1)	29 (1·7)
tSAH	1002 (58)	194 (11·2)	316 (18·3)	73 (4·2)	124 (7·2)	160 (9·3)	135 (7·8)
Daily therapies any day							
Daily TIL, max	4 (1, 10)	0 (0, 2)	5 (2, 10)	6 (2, 12)	5 (0, 9)	8 (4, 13)	9 (4, 15)
Head elevation for ICP control	1066 (61·7)	160 (36·5)	347 (68·6)	80 (67·2)	135 (66·8)	192 (74·7)	152 (73·8)
Nursed flat for CPP management	139 (8)	4 (0·9)	62 (12·3)	19 (16)	12 (5·9)	22 (8·6)	20 (9·7)
Fluid loading for maintenance of cerebral perfusion	586 (33·9)	42 (9·6)	175 (34·6)	49 (41·2)	79 (39·1)	140 (54·5)	101 (49)
Vasopressor therapy	815 (47·2)	54 (12·3)	267 (52·8)	71 (59·7)	103 (51)	180 (70)	140 (68)
Decompressive craniectomy	155 (9)	9 (2·1)	30 (5·9)	22 (18·5)	21 (10·4)	40 (15·6)	33 (16)
Neuromuscular block	311 (18)	23 (5·3)	107 (21·1)	30 (25·2)	32 (15·8)	58 (22·6)	61 (29·6)
Temperature control	901 (52·1)	37 (8·4)	315 (62·3)	69 (58)	105 (52)	176 (68·5)	199 (96·6)
No	778 (45)	279 (63·7)	196 (38·7)	47 (39·5)	83 (41·1)	97 (37·7)	76 (36·9)
Treatment of temperature >38 °C or spontaneous temperature <34·5 °C	465 (26·9)	33 (7·5)	202 (39·9)	45 (37·8)	62 (30·7)	84 (32·7)	39 (18·9)
Mild hypothermia for ICP control (>35 °C)	80 (4·6)	2 (0·5)	22 (4·3)	6 (5)	8 (4)	19 (7·4)	23 (11·2)
Hypothermia <35 °C	92 (5·3)		23 (4·5)	4 (3·4)	9 (4·5)	18 (7)	38 (18·4)
NA	313 (18·1)	124 (28·3)	63 (12·5)	17 (14·3)	40 (19·8)	39 (15·2)	30 (14·6)

	All patients	α	β	γ	δ	ε	ζ
Hypertonic saline for ICP control							
No	1116 (64·6)	305 (69·6)	347 (68·6)	82 (68·9)	135 (66·8)	144 (56)	103 (50)
< 0·3g/kg/24 h	195 (11·3)	5 (1·1)	61 (12·1)	14 (11·8)	20 (9·9)	46 (17·9)	49 (23·8)
> 0·3 g/kg/24 h	104 (6)	4 (0·9)	35 (6·9)	6 (5)	7 (3·5)	28 (10·9)	24 (11·7)
NA	313 (18·1)	124 (28·3)	63 (12·5)	17 (14·3)	40 (19·8)	39 (15·2)	30 (14·6)
Mannitol for ICP control							
No	1211 (70·1)	305 (69·6)	392 (77·5)	92 (77·3)	138 (68·3)	165 (64·2)	119 (57·8)
< 2g/kg/24 h	165 (9·5)	9 (2·1)	46 (9·1)	9 (7·6)	20 (9·9)	41 (16)	40 (19·4)
> 2g/kg/24 h	39 (2·3)		5 (1)	1 (0·8)	4 (2)	12 (4·7)	17 (8·3)
NA	313 (18·1)	124 (28·3)	63 (12·5)	17 (14·3)	40 (19·8)	39 (15·2)	30 (14·6)
Sedation therapy							
No	306 (17·7)	201 (45·9)	47 (9·3)	10 (8·4)	28 (13·9)	5 (1·9)	15 (7·3)
Low dose required for mechanical ventilation	531 (30·7)	91 (20·8)	199 (39·3)	40 (33·6)	66 (32·7)	91 (35·4)	44 (21·4)
Higher dose sedation for ICP control	276 (16)	8 (1·8)	79 (15·6)	32 (26·9)	39 (19·3)	70 (27·2)	48 (23·3)
Metabolic suppression for ICP control w high dose barbiturates or propofol	302 (17·5)	14 (3·2)	118 (23·3)	20 (16·8)	29 (14·4)	52 (20·2)	69 (33·5)
NA	313 (18·1)	124 (28·3)	63 (12·5)	17 (14·3)	40 (19·8)	39 (15·2)	30 (14·6)
CSF Drainage therapy							
No	1309 (75·8)	357 (81·5)	402 (79·4)	90 (75·6)	133 (65·8)	180 (70)	147 (71·4)
< 120 ml/day	68 (3·9)	3 (0·7)	13 (2·6)	6 (5)	13 (6·4)	17 (6·6)	16 (7·8)
>= 120 ml/day	134 (7·8)	5 (1·1)	45 (8·9)	8 (6·7)	19 (9·4)	33 (12·8)	24 (11·7)
NA	217 (12·6)	73 (16·7)	46 (9·1)	15 (12·6)	37 (18·3)	27 (10·5)	19 (9·2)
Hyperventilation therapy for ICP control							
No	829 (48)	285 (65·1)	231 (45·7)	45 (37·8)	90 (44·6)	90 (35)	88 (42·7)
$PaCO_2$ 4·6-5·3 kPa	377 (21·8)	25 (5·7)	138 (27·3)	38 (31·9)	54 (26·7)	81 (31·5)	41 (19·9)
$PaCO_2$ 4·0-4·5 kPa	161 (9·3)	4 (0·9)	62 (12·3)	15 (12·6)	14 (6·9)	35 (13·6)	31 (15)
$PaCO_2$ < 4·0 kPa	47 (2·7)		12 (2·4)	4 (3·4)	3 (1·5)	12 (4·7)	16 (7·8)

	All patients	α	β	γ	δ	ε	ζ
NA	314 (18·2)	124 (28·3)	63 (12·5)	17 (14·3)	41 (20·3)	39 (15·2)	30 (14·6)
Biomarkers, highest							
UCH-L1 [pg/mL]	353·4 (159·8, 738·3)	123·16 (70·89, 203·02)	451·73 (227·95, 775·90)	295·4 (165·65, 545·05)	420·68 (181·78, 835·33)	701·42 (346·7, 1046·7)	717·47 (390·53, 1294·93)
S100B [µg/L]	0·29 (0·16, 0·54)	0·16 (0·1, 0·25)	0·33 (0·21, 0·56)	0·25 (0·17, 0·35)	0·32 (0·16, 0·63)	0·44 (0·25, 0·67)	0·58 (0·256, 0·90)
Tau [pg/mL]	8·48 (3·98, 18·79)	3·345 (2·0625, 5·65)	10·62 (5·41, 19·99)	7·49 (4·08, 13·24)	8·61 (4·74, 17·09)	16·26 (8·58, 30·25)	18·08 (10·66, 35·26)
NFL [pg/mL]	76·5 (34·8, 177·3)	25·63 (13·58, 45·96)	95·33 (52·65, 183·54)	86·9 (44·91, 180·72)	71·68 (34·63, 201·01)	146·68 (75·35, 248·74)	191·02 (90·37, 367·59)
GFAP [ng/mL]	20·2 (6·7, 51·5)	5·9 (2·1, 14·1)	27·345 (10·55, 58·30)	16·1 (7·36, 29·24)	20·95 (7·30, 60·20)	48·04 (21·41, 73·57)	44·13 (15·74, 83·11)
NSE [ng/mL]	23·26 (16·61, 34·11)	17·48 (13·01, 22·59)	24·8 (18·37, 34·11)	20·43 (16·28, 28·18)	25·43 (17·57, 35·33)	28·16 (20·30, 41·52)	31·36 (23·43, 47·87)
IMPACT predicted mortality, median, %	22·1 (10·7, 40·2)	12·9 (7·2, 18·6)	22·1 (12·9, 35·2)	22·1 (15·6, 45·5)	26 (12·9, 40·2)	30·4 (18·6, 50·9)	40·2 (22·1, 60·2)
Mortality, observed, n (%)	388 (22·5)	16 (3·7)	85 (16·8)	22 (18·5)	54 (26·7)	77 (30)	134 (65)
IMPACT predicted unfavorable outcome, %	43·8 (21·8, 68·5)	26·5 (14·3, 37·6)	43·8 (26·5, 62·7)	43·8 (31·8, 73·8)	50·2 (26·5, 68·5)	56·6 (37·6, 78·4)	68·5 (43·8, 85)
Unfavorable outcome, observed, n (%)	779 (45·1)	78 (17·8)	211 (41·7)	58 (48·7)	92 (45·5)	166 (64·6)	174 (84·5)

Description of patients, overall and stratified by trajectory· Data are in median (interquartile range) or n(%).GOS-E= Glasgow outcome scale extended, ASA-PS=American society of anaesthesiologists' physical status, ISS=Injury Severity Score, ICP=Intracranial pressure, GCS=Glasgow Coma Scale, MAP=Mean arterial pressure, $PaCO_2$=arterial partial pressure of carbon dioxide, PaO_2=arterial partial pressure of oxygen, SpO_2=Oxygen saturation, CT=Computed tomography, TAI=Traumatic axonal injury, aSDH=acute subdural hematoma, EDH=Epidural hematoma, tSAH=traumatic subarachnoid hemorrhage, TIL=Therapy Intensity Level, CPP=Cerebral perfusion pressure, CSF=Cerebrospinal fluid, UCH-L1=Ubiquitine carboxy-terminal hydrolase L1, S100B=S100 calcium-binding protein B, NFL=Neurofilament light, GFAP=Glial fibrillary atrial protein, NSE=Neuron-specific endolase, , IMPACT= International Mission for Prognosis and Analysis of Clinical trials in TBI, NA=not applicable (missing).

Supplementary Table 4: Probabilities (%) of cluster membership for patients assigned to each cluster, expressed as mean (SD).

Cluster	Mean (SD) probability of cluster assignment (%)
α	98·9 (4·6)
β	97·8 (9·3)
γ	99·3 (2·6)
δ	98·8 (6·1)
ε	97·0 (10·5)
ζ	98·6 (8·4)

Supplementary Table 5: Most prominent features day by day.

Admission	Day 1	Day 2	Day 3	Day 4	Day 5	Day 6	Day 7
Lactate	Δ Glucose	Δ Glucose	Δ Glucose	Δ Glucose	Δ Glucose	Δ Glucose	Δ Glucose
SpO_2 mean	Creatinine	Creatinine	Δ SpO_2	Tau	Tau	Tau	GFAP
GCS Motor score	NFL	Δ Sodium	Tau	S100B	GFAP	GFAP	UCH-L1
pH mean	CSF drainage volume	Δ SpO_2	Creatinine	UCH-L1	UCH-L1	S100B	NFL
BE	ICP mean	NFL	UCH-L1	GFAP	SpO_2 mean	UCH-L1	Tau
Intubation	GFAP	Tau	NFL	NFL	S100B	NSE	NSE
GCS Verbal score	Δ SpO_2	SpO_2 mean	S100B	Creatinine	Δ SpO_2	Δ pH	S100B
$PaCO_2$ mean	Tau	UCH-L1	ICP mean	NSE	Creatinine	SpO_2 mean	SpO_2 mean
GCS Eye score	UCH-L1	S100B	SpO_2 mean	Δ SpO_2	Δ pH	Δ PaO_2	Δ pH
Body temperature mean	Δ Sodium	ICP mean	GFAP	SpO_2 mean	NSE	Δ SpO_2	Δ SpO_2

Most prominent features day by day, expressed as having highest mean mutual information between trajectory index and feature in the six cluster models. SpO_2=Oxygen saturation. GCS=Glasgow Coma Scale. BE=Base excess. $PaCO_2$=Arterial partial pressure of carbon dioxide. NFL=Neurofilament light. CSF=Cerebrospinal fluid. ICP=Intracranial pressure. GFAP=Glial fibrillary acidic protein. UCH-L1=Ubiquitin carboxy-terminal hydrolase L1. S100B=S100 calcium-binding protein B. NSE=Neuron-specific enolase. PaO_2=Arterial partial pressure of oxygen.

Supplementary Table 6: Probabilities (%) of following the identified trajectories (column) if assigned to a certain cluster (row) in a previously described clustering on admission features.

Trajectory	α	β	γ	δ	ε	ζ
A	57·14	21·53	5·03	8·85	3·82	3·62
B	16·41	29·77	6·49	12·98	23·28	11·07
C	10·42	31·25	10·42	18·75	4·17	25·00
D	18·37	33·53	7·58	9·91	20·99	9·62
E	5·00	32·78	9·72	9·72	23·61	19·17
F	11·47	33·49	5·05	21·10	8·26	20·64

The admission clustering was performed on the same cohort as in the present study. Cluster A corresponds to a cluster with mild TBI and normal systemic metabolic profile, cluster B moderate TBI with normal systemic metabolic profile, cluster C moderate TBI but deranged metabolism, cluster D, severe TBI with normal metabolism, cluster E severe TBI with deranged metabolism and a distinct TBI profile, and cluster F severe TBI and deranged metabolism with mainly a systemic shock picture. This table is illustrated in Supplementary Fig 7.

Supplementary Table 7: Explained variance (Nagelkerke's pseudo-R^2) in outcome predictions by the IMPACT lab model features, with addition of cluster assignments, mean and standard deviations of 1,000 bootstraps.

			Mortality		Unfavorable outcome	
N clusters	**Mortality**	**Unfavorable outcome**	**IMPACT lab model (no cluster indices)**	**IMPACT lab model + cluster index**	**IMPACT lab model (no cluster indices)**	**IMPACT lab model + cluster index**
1	*NA*	*NA*	0·44	*NA*	0·36	*NA*
2	0·13 (0·02)	0·14 (0·02)		0·43 (0·03)		0·36 (0·02)
3	0·21 (0·02)	0·17 (0·02)		0·48 (0·02)		0·39 (0·02)
4	0·26 (0·03)	0·20 (0·02)		0·51 (0·02)		0·41 (0·02)
5	0·25 (0·03)	0·23 (0·02)		0·50 (0·02)		0·41 (0·02)
6	0·25 (0·02)	0·23 (0·02)		0·51 (0·02)		0·42 (0·02)
7	0·30 (0·02)	0·27 (0·02)		0·51 (0·02)		0·42 (0·02)
8	0·28 (0·03)	0·25 (0·02)		0·51 (0·02)		0·42 (0·02)
9	0·28 (0·03)	0·28 (0·02)		0·51 (0·02)		0·44 (0·02)
10	0·27 (0·02)	0·26 (0·02)		0·50 (0·02)		0·43 (0·02)
11	0·29 (0·02)	0·26 (0·02)		0·51 (0·02)		0·43 (0·02)
12	0·30 (0·03)	0·30 (0·02)		0·53 (0·02)		0·45 (0·02)

Explained variance (Nagelkerke's pseudo-R^2) in outcome predictions of the IMPACT lab model, including the features age, Glasgow coma scale motor score, pupillary reactivity, Marshall CT classification, presence of traumatic subarachnoid hemorrhage, presence of epidural hematoma, hypoxic and hypotensive events, serum glucose and hemoglobin. Logistic regression was performed – first, only with the original IMPACT variables as predictors, and second, with the IMPACT model variables and by adding cluster assignment for three to twelve clusters. Twelve clusters lead to the highest increase in pseudo-R^2, both in mortality prediction (0·44 to 0·53) and in unfavorable outcome prediction (0·36 to 0·45). The results are index-corrected to adjust for the addition of features in the prediction model. The logistic regression was performed 1,000 times for each number of clusters, on bootstrapped subpopulations of the cohort. Values presented in the table are mean (standard deviation).

Supplementary Figures

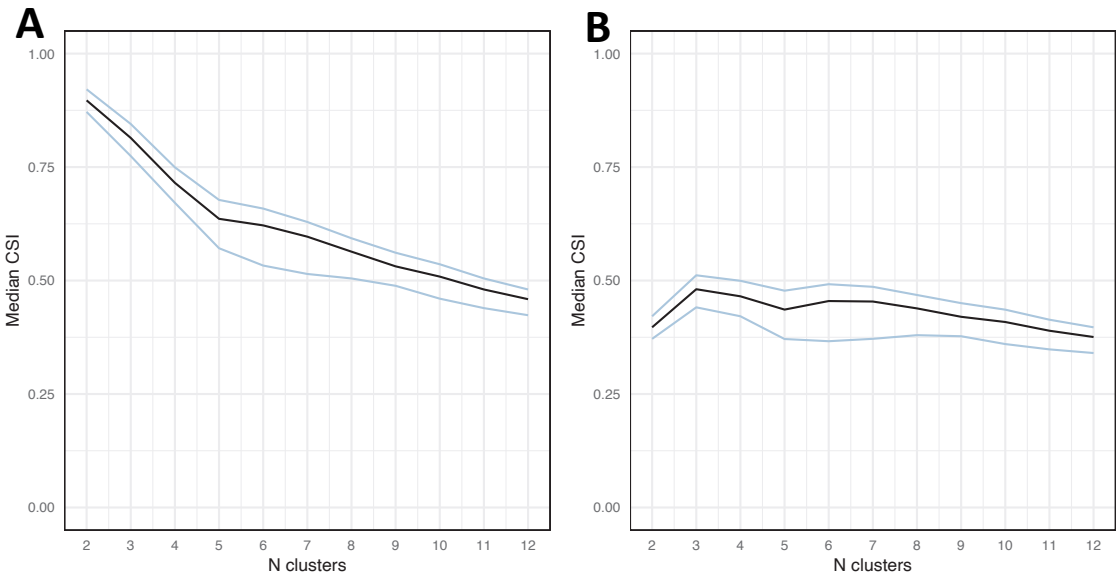

Supplementary Figure 1: Median cluster similarity index (CSI) for 25 models vs number of clusters, IQR indicated in blue. The CSI is a measure of how many times all pairwise combinations of patients appear in the same cluster, or in different clusters in all combinations of pairwise models, for each number of clusters. **A:** A discrete plateau is seen in the decreasing CSI curve: at five to six clusters. **B:** A penalty of 1/n(clusters) is subtracted from the median CSI to adjust for the higher probability of high CSIs in the case of fewer clusters. A peak in CSI can be seen at three clusters, with a discrete plateau between six and seven clusters. This can be interpreted as no cluster solution seem to produce more stable results than any other.

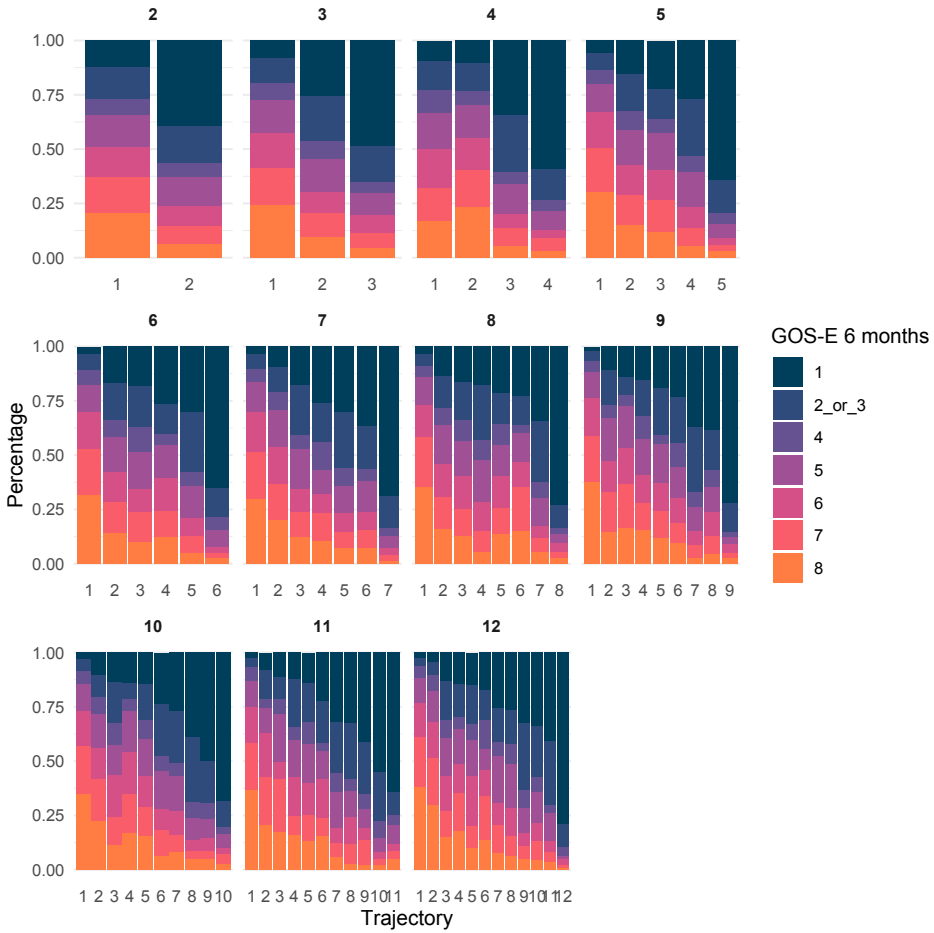

Supplementary Figure 2: 6-month outcome in incremental models, stratified per cluster. Outcome is represented by Glasgow outcome scale extended (GOS-E). Although GOS-E was not known when creating the clusters, the outcome profiles were different between clusters, in all models of two to twelve clusters.

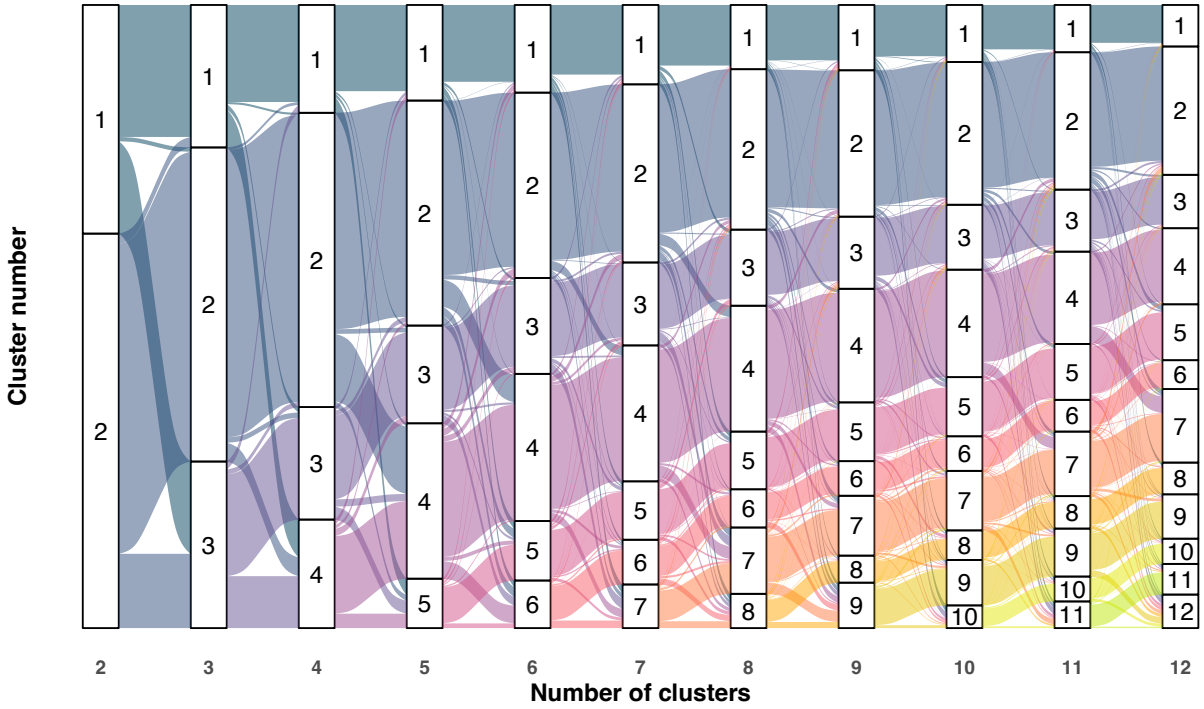

Supplementary Figure 3: Distribution of patients in incremental models. Models were created by, as a first step, randomly assigning patients to two clusters. In the next step, a new cluster with randomly assigned patients from both previous clusters was added, and the cluster algorithm was repeated until stability (i.e., when the probability change of belonging to a certain cluster was under a set threshold of 10^6, or a maximum of 1000 iterations). This was repeated for up to twelve clusters. This figure illustrates how the cluster assignments are changing when extending the model with an additional cluster.

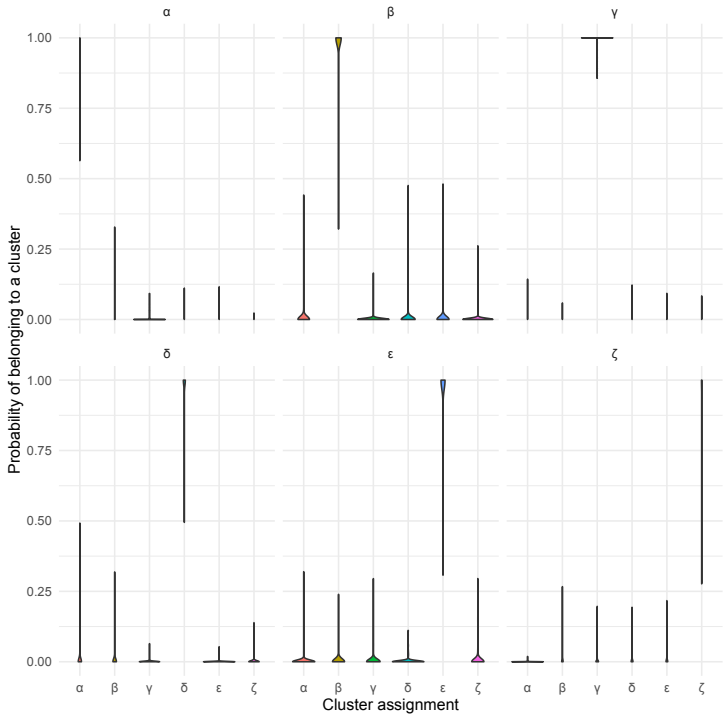

Supplementary Figure 4: Probability of belonging to a trajectory cluster stratified by cluster assignment. Violin plots show the distributions of probabilities. The cluster labels on the x axis represents the assigned cluster, and each subplot represents the probability of being assigned to that particular cluster. Almost all patients have a very high probability of belonging to the cluster assigned, indicating good stability in the clustering.

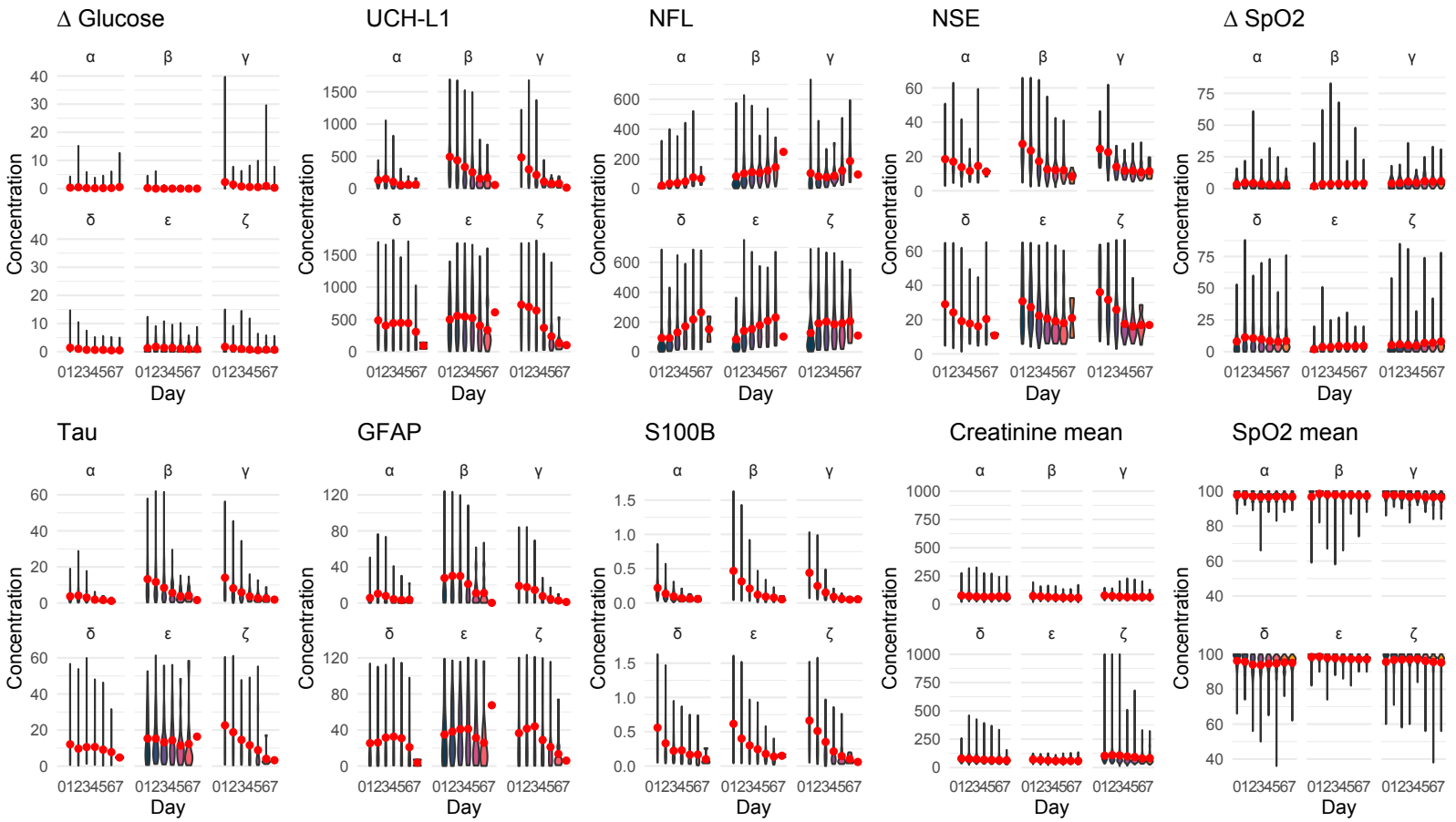

Supplementary Figure 5: Distributions of the most important features on all days by cluster. The features with highest mutual information, distributions per day and cluster. Daily cluster means are represented by a red point. UCH-L1=Ubiquitin carboxy-terminal hydrolase L1. NFL=Neurofilament light. NSE=Neuron-specific enolase. SpO2=Oxygen saturation. GFAP=Glial fibrillary acidic protein. S100B=S100 calcium-binding protein B.

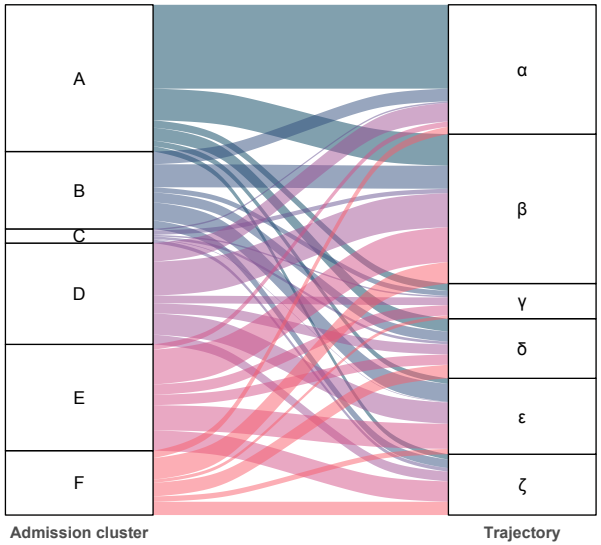

Supplementary Figure 6: Probabilities of following a certain trajectory in clusters identified at admission. The admission clusters were described in a previous study and developed in the same cohort. The width of each line represents the proportion of patients in each admission cluster following a trajectory. Admission cluster A (mild TBI) had a large proportion of patients following trajectory α, while all other admission clusters (B (moderate TBI with normal metabolism), C (moderate TBI with deranged metabolism), D (severe TBI with normal metabolism), E (severe TBI with deranged metabolism), and F (the cluster with severe TBI and most deranged metabolism)) most likely followed β. In addition, 25% of patients in admission cluster C followed trajectory ζ, 24% in admission cluster E followed ε, and 21% of admission cluster F followed trajectory ζ. For more details, see Table 3.

The CENTER-TBI participants and investigators

Cecilia Åkerlund[1], Krisztina Amrein[2], Nada Andelic[3], Lasse Andreassen[4], Audny Anke[5], Anna Antoni[6], Gérard Audibert[7], Philippe Azouvi[8], Maria Luisa Azzolini[9], Ronald Bartels[10], Pál Barzó[11], Romuald Beauvais[12], Ronny Beer[13], Bo-Michael Bellander[14], Antonio Belli[15], Habib Benali[16], Maurizio Berardino[17], Luigi Beretta[9], Morten Blaabjerg[18], Peter Bragge[19], Alexandra Brazinova[20], Vibeke Brinck[21], Joanne Brooker[22], Camilla Brorsson[23], Andras Buki[24], Monika Bullinger[25], Manuel Cabeleira[26], Alessio Caccioppola[27], Emiliana Calappi [27], Maria Rosa Calvi[9], Peter Cameron[28], Guillermo Carbayo Lozano[29], Marco Carbonara[27], Simona Cavallo[17], Giorgio Chevallard[30], Arturo Chieregato[30], Giuseppe Citerio[31, 32], Hans Clusmann[33], Mark Coburn[34], Jonathan Coles[35], Jamie D. Cooper[36], Marta Correia[37], Amra Čović [38], Nicola Curry[39], Endre Czeiter[24], Marek Czosnyka[26], Claire Dahyot-Fizelier[40], Paul Dark[41], Helen Dawes[42], Véronique De Keyser[43], Vincent Degos[16], Francesco Della Corte[44], Hugo den Boogert[10], Bart Depreitere[45], Đula Đilvesi [46], Abhishek Dixit[47], Emma Donoghue[22], Jens Dreier[48], Guy-Loup Dulière[49], Ari Ercole[47], Patrick Esser[42], Erzsébet Ezer[50], Martin Fabricius[51], Valery L. Feigin[52], Kelly Foks[53], Shirin Frisvold[54], Alex Furmanov[55], Pablo Gagliardo[56], Damien Galanaud[16], Dashiell Gantner[28], Guoyi Gao[57], Pradeep George[58], Alexandre Ghuysen[59], Lelde Giga[60], Ben Glocker[61], Jagoš Golubovic[46], Pedro A. Gomez [62], Johannes Gratz[63], Benjamin Gravesteijn[64], Francesca Grossi[44], Russell L. Gruen[65], Deepak Gupta[66], Juanita A. Haagsma[64], Iain Haitsma[67], Raimund Helbok[13], Eirik Helseth[68], Lindsay Horton [69], Jilske Huijben[64], Peter J. Hutchinson[70], Bram Jacobs[71], Stefan Jankowski[72], Mike Jarrett[21], Ji-yao Jiang[58], Faye Johnson[73], Kelly Jones[52], Mladen Karan[46], Angelos G. Kolias[70], Erwin Kompanje[74], Daniel Kondziella[51], Evgenios Kornaropoulos[47], Lars-Owe Koskinen[75], Noémi Kovács[76], Ana Kowark[77], Alfonso Lagares[62], Linda Lanyon[58], Steven Laureys[78], Fiona Lecky[79, 80], Didier Ledoux[78], Rolf Lefering[81], Valerie Legrand[82], Aurelie Lejeune[83], Leon Levi[84], Roger Lightfoot[85], Hester Lingsma[64], Andrew I.R. Maas[43], Ana M. Castaño-León[62], Marc Maegele[86], Marek Majdan[20], Alex Manara[87], Geoffrey Manley[88], Costanza Martino[89], Hugues Maréchal[49], Julia Mattern[90], Catherine McMahon[91], Béla Melegh[92], David Menon[47], Tomas Menovsky[43], Ana Mikolic[64], Benoit Misset[78], Visakh Muraleedharan[58], Lynnette Murray[28], Ancuta Negru[93], David Nelson[1], Virginia Newcombe[47], Daan Nieboer[64], József Nyirádi[2], Otesile Olubukola[79], Matej Oresic[94], Fabrizio Ortolano[27], Aarno Palotie[95, 96, 97], Paul M. Parizel[98], Jean-François Payen[99], Natascha Perera[12], Vincent Perlbarg[16], Paolo Persona[100], Wilco Peul[101], Anna Piippo-Karjalainen[102], Matti Pirinen[95], Dana Pisica[64], Horia Ples[93], Suzanne Polinder[64], Inigo Pomposo[29], Jussi P. Posti [103], Louis Puybasset[104], Andreea Radoi [105], Arminas Ragauskas[106], Rahul Raj[102], Malinka Rambadagalla[107], Isabel Retel Helmrich[64], Jonathan Rhodes[108], Sylvia Richardson[109], Sophie Richter[47], Samuli Ripatti[95], Saulius

Rocka[106], Cecilie Roe[110], Olav Roise[111,112], Jonathan Rosand[113], Jeffrey V. Rosenfeld[114], Christina Rosenlund[115], Guy Rosenthal[55], Rolf Rossaint[77], Sandra Rossi[100], Daniel Rueckert[61] Martin Rusnák[116], Juan Sahuquillo[105], Oliver Sakowitz[90, 117], Renan Sanchez-Porras[117], Janos Sandor[118], Nadine Schäfer[81], Silke Schmidt[119], Herbert Schoechl[120], Guus Schoonman[121], Rico Frederik Schou[122], Elisabeth Schwendenwein[6], Charlie Sewalt[64], Ranjit D. Singh[101], Toril Skandsen[123, 124], Peter Smielewski[26], Abayomi Sorinola[125], Emmanuel Stamatakis[47], Simon Stanworth[39], Robert Stevens[126], William Stewart[127], Ewout W. Steyerberg[64, 128], Nino Stocchetti[129], Nina Sundström[130], Riikka Takala[131], Viktória Tamás[125], Tomas Tamosuitis[132], Mark Steven Taylor[20], Braden Te Ao[52], Olli Tenovuo[103], Alice Theadom[52], Matt Thomas[87], Dick Tibboel[133], Marjolein Timmers[74], Christos Tolias[134], Tony Trapani[28], Cristina Maria Tudora[93], Andreas Unterberg[90], Peter Vajkoczy [135], Shirley Vallance[28], Egils Valeinis[60], Zoltán Vámos[50], Mathieu van der Jagt[136], Gregory Van der Steen[43], Joukje van der Naalt[71], Jeroen T.J.M. van Dijck [101], Inge A. M. van Erp[101], Thomas A. van Essen[101], Wim Van Hecke[137], Caroline van Heugten[138], Dominique Van Praag[139], Ernest van Veen[64], Thijs Vande Vyvere[137], Roel P. J. van Wijk[101], Alessia Vargiolu[32], Emmanuel Vega[83], Kimberley Velt[64], Jan Verheyden[137], Paul M. Vespa[140], Anne Vik[123, 141], Rimantas Vilcinis[132], Victor Volovici[67], Nicole von Steinbüchel[38], Daphne Voormolen[64], Petar Vulekovic[46], Kevin K.W. Wang[142], Daniel Whitehouse[47], Eveline Wiegers[64], Guy Williams[47], Lindsay Wilson[69], Stefan Winzeck[47], Stefan Wolf[143], Zhihui Yang[113], Peter Ylén[144], Alexander Younsi[90], Frederick A. Zeiler[47,145], Veronika Zelinkova[20], Agate Ziverte[60], Tommaso Zoerle[27]

[1] Department of Physiology and Pharmacology, Section of Perioperative Medicine and Intensive Care, Karolinska Institutet, Stockholm, Sweden

[2] János Szentágothai Research Centre, University of Pécs, Pécs, Hungary

[3] Division of Clinical Neuroscience, Department of Physical Medicine and Rehabilitation, Oslo University Hospital and University of Oslo, Oslo, Norway

[4] Department of Neurosurgery, University Hospital Northern Norway, Tromso, Norway

[5] Department of Physical Medicine and Rehabilitation, University Hospital Northern Norway, Tromso, Norway

[6] Trauma Surgery, Medical University Vienna, Vienna, Austria

[7] Department of Anesthesiology & Intensive Care, University Hospital Nancy, Nancy, France

[8] Raymond Poincare hospital, Assistance Publique – Hopitaux de Paris, Paris, France

[9] Department of Anesthesiology & Intensive Care, S Raffaele University Hospital, Milan, Italy

[10] Department of Neurosurgery, Radboud University Medical Center, Nijmegen, The Netherlands

[11] Department of Neurosurgery, University of Szeged, Szeged, Hungary

[12] International Projects Management, ARTTIC, Munchen, Germany

[13] Department of Neurology, Neurological Intensive Care Unit, Medical University of Innsbruck, Innsbruck, Austria

[14] Department of Neurosurgery & Anesthesia & intensive care medicine, Karolinska University Hospital, Stockholm, Sweden

[15] NIHR Surgical Reconstruction and Microbiology Research Centre, Birmingham, UK

[16] Anesthesie-Réanimation, Assistance Publique – Hopitaux de Paris, Paris, France

[17] Department of Anesthesia & ICU, AOU Città della Salute e della Scienza di Torino - Orthopedic and Trauma Center, Torino, Italy

[18] Department of Neurology, Odense University Hospital, Odense, Denmark

[19] BehaviourWorks Australia, Monash Sustainability Institute, Monash University, Victoria, Australia

[20] Department of Public Health, Faculty of Health Sciences and Social Work, Trnava University, Trnava, Slovakia

[21] Quesgen Systems Inc., Burlingame, California, USA

[22] Australian & New Zealand Intensive Care Research Centre, Department of Epidemiology and Preventive Medicine, School of Public Health and Preventive Medicine, Monash University, Melbourne, Australia

[23] Department of Surgery and Perioperative Science, Umeå University, Umeå, Sweden

[24] Department of Neurosurgery, Medical School, University of Pécs, Hungary and Neurotrauma Research Group, János Szentágothai Research Centre, University of Pécs, Hungary

[25] Department of Medical Psychology, Universitätsklinikum Hamburg-Eppendorf, Hamburg, Germany

[26] Brain Physics Lab, Division of Neurosurgery, Dept of Clinical Neurosciences, University of Cambridge, Addenbrooke's Hospital, Cambridge, UK

[27] Neuro ICU, Fondazione IRCCS Cà Granda Ospedale Maggiore Policlinico, Milan, Italy

[28] ANZIC Research Centre, Monash University, Department of Epidemiology and Preventive Medicine, Melbourne, Victoria, Australia

[29] Department of Neurosurgery, Hospital of Cruces, Bilbao, Spain

[30] NeuroIntensive Care, Niguarda Hospital, Milan, Italy

[31] School of Medicine and Surgery, Università Milano Bicocca, Milano, Italy

[32] NeuroIntensive Care, ASST di Monza, Monza, Italy

[33]Department of Neurosurgery, Medical Faculty RWTH Aachen University, Aachen, Germany

[34] Department of Anesthesiology and Intensive Care Medicine, University Hospital Bonn, Bonn, Germany

[35] Department of Anesthesia & Neurointensive Care, Cambridge University Hospital NHS Foundation Trust, Cambridge, UK

[36] School of Public Health & PM, Monash University and The Alfred Hospital, Melbourne, Victoria, Australia

[37] Radiology/MRI department, MRC Cognition and Brain Sciences Unit, Cambridge, UK

[38] Institute of Medical Psychology and Medical Sociology, Universitätsmedizin Göttingen, Göttingen, Germany

[39] Oxford University Hospitals NHS Trust, Oxford, UK

[40] Intensive Care Unit, CHU Poitiers, Potiers, France

[41] University of Manchester NIHR Biomedical Research Centre, Critical Care Directorate, Salford Royal Hospital NHS Foundation Trust, Salford, UK

[42] Movement Science Group, Faculty of Health and Life Sciences, Oxford Brookes University, Oxford, UK

[43] Department of Neurosurgery, Antwerp University Hospital and University of Antwerp, Edegem, Belgium

[44] Department of Anesthesia & Intensive Care, Maggiore Della Carità Hospital, Novara, Italy

[45] Department of Neurosurgery, University Hospitals Leuven, Leuven, Belgium

[46] Department of Neurosurgery, Clinical centre of Vojvodina, Faculty of Medicine, University of Novi Sad, Novi Sad, Serbia

[47] Division of Anaesthesia, University of Cambridge, Addenbrooke's Hospital, Cambridge, UK

[48] Center for Stroke Research Berlin, Charité – Universitätsmedizin Berlin, corporate member of Freie Universität Berlin, Humboldt-Universität zu Berlin, and Berlin Institute of Health, Berlin, Germany

[49] Intensive Care Unit, CHR Citadelle, Liège, Belgium

[50] Department of Anaesthesiology and Intensive Therapy, University of Pécs, Pécs, Hungary

[51] Departments of Neurology, Clinical Neurophysiology and Neuroanesthesiology, Region Hovedstaden Rigshospitalet, Copenhagen, Denmark

[52] National Institute for Stroke and Applied Neurosciences, Faculty of Health and Environmental Studies, Auckland University of Technology, Auckland, New Zealand

[53] Department of Neurology, Erasmus MC, Rotterdam, the Netherlands

[54] Department of Anesthesiology and Intensive care, University Hospital Northern Norway, Tromso, Norway

[55] Department of Neurosurgery, Hadassah-hebrew University Medical center, Jerusalem, Israel

[56] Fundación Instituto Valenciano de Neurorrehabilitación (FIVAN), Valencia, Spain

[57] Department of Neurosurgery, Shanghai Renji hospital, Shanghai Jiaotong University/school of medicine, Shanghai, China

[58] Karolinska Institutet, INCF International Neuroinformatics Coordinating Facility, Stockholm, Sweden

[59] Emergency Department, CHU, Liège, Belgium

[60] Neurosurgery clinic, Pauls Stradins Clinical University Hospital, Riga, Latvia

[61] Department of Computing, Imperial College London, London, UK

[62] Department of Neurosurgery, Hospital Universitario 12 de Octubre, Madrid, Spain

[63] Department of Anesthesia, Critical Care and Pain Medicine, Medical University of Vienna, Austria

[64] Department of Public Health, Erasmus Medical Center-University Medical Center, Rotterdam, The Netherlands

[65] College of Health and Medicine, Australian National University, Canberra, Australia

[66] Department of Neurosurgery, Neurosciences Centre & JPN Apex trauma centre, All India Institute of Medical Sciences, New Delhi-110029, India

[67] Department of Neurosurgery, Erasmus MC, Rotterdam, the Netherlands

[68] Department of Neurosurgery, Oslo University Hospital, Oslo, Norway

[69] Division of Psychology, University of Stirling, Stirling, UK

[70] Division of Neurosurgery, Department of Clinical Neurosciences, Addenbrooke's Hospital & University of Cambridge, Cambridge, UK

[71] Department of Neurology, University of Groningen, University Medical Center Groningen, Groningen, Netherlands

[72] Neurointensive Care , Sheffield Teaching Hospitals NHS Foundation Trust, Sheffield, UK

[73] Salford Royal Hospital NHS Foundation Trust Acute Research Delivery Team, Salford, UK

[74] Department of Intensive Care and Department of Ethics and Philosophy of Medicine, Erasmus Medical Center, Rotterdam, The Netherlands

[75] Department of Clinical Neuroscience, Neurosurgery, Umeå University, Umeå, Sweden

[76] Hungarian Brain Research Program - Grant No. KTIA_13_NAP-A-II/8, University of Pécs, Pécs, Hungary

[77] Department of Anaesthesiology, University Hospital of Aachen, Aachen, Germany

[78] Cyclotron Research Center , University of Liège, Liège, Belgium

[79] Centre for Urgent and Emergency Care Research (CURE), Health Services Research Section, School of Health and Related Research (ScHARR), University of Sheffield, Sheffield, UK

[80] Emergency Department, Salford Royal Hospital, Salford UK

[81] Institute of Research in Operative Medicine (IFOM), Witten/Herdecke University, Cologne, Germany

[82] VP Global Project Management CNS, ICON, Paris, France

[83] Department of Anesthesiology-Intensive Care, Lille University Hospital, Lille, France

[84] Department of Neurosurgery, Rambam Medical Center, Haifa, Israel

[85] Department of Anesthesiology & Intensive Care, University Hospitals Southhampton NHS Trust, Southhampton, UK

[86] Cologne-Merheim Medical Center (CMMC), Department of Traumatology, Orthopedic Surgery and Sportmedicine, Witten/Herdecke University, Cologne, Germany

[87] Intensive Care Unit, Southmead Hospital, Bristol, Bristol, UK

[88] Department of Neurological Surgery, University of California, San Francisco, California, USA

[89] Department of Anesthesia & Intensive Care,M. Bufalini Hospital, Cesena, Italy

[90] Department of Neurosurgery, University Hospital Heidelberg, Heidelberg, Germany

[91] Department of Neurosurgery, The Walton centre NHS Foundation Trust, Liverpool, UK

[92] Department of Medical Genetics, University of Pécs, Pécs, Hungary

[93] Department of Neurosurgery, Emergency County Hospital Timisoara , Timisoara, Romania

[94] School of Medical Sciences, Örebro University, Örebro, Sweden

[95] Institute for Molecular Medicine Finland, University of Helsinki, Helsinki, Finland

[96] Analytic and Translational Genetics Unit, Department of Medicine; Psychiatric & Neurodevelopmental Genetics Unit, Department of Psychiatry; Department of Neurology, Massachusetts General Hospital, Boston, MA, USA

[97] Program in Medical and Population Genetics; The Stanley Center for Psychiatric Research, The Broad Institute of MIT and Harvard, Cambridge, MA, USA

[98] Department of Radiology, University of Antwerp, Edegem, Belgium

[99] Department of Anesthesiology & Intensive Care, University Hospital of Grenoble, Grenoble, France

[100] Department of Anesthesia & Intensive Care, Azienda Ospedaliera Università di Padova, Padova, Italy

[101] Dept. of Neurosurgery, Leiden University Medical Center, Leiden, The Netherlands and Dept. of Neurosurgery, Medical Center Haaglanden, The Hague, The Netherlands

[102] Department of Neurosurgery, Helsinki University Central Hospital

[103] Division of Clinical Neurosciences, Department of Neurosurgery and Turku Brain Injury Centre, Turku University Hospital and University of Turku, Turku, Finland

[104] Department of Anesthesiology and Critical Care, Pitié -Salpêtrière Teaching Hospital, Assistance Publique, Hôpitaux de Paris and University Pierre et Marie Curie, Paris, France

[105] Neurotraumatology and Neurosurgery Research Unit (UNINN), Vall d'Hebron Research Institute, Barcelona, Spain

[106] Department of Neurosurgery, Kaunas University of technology and Vilnius University, Vilnius, Lithuania

[107] Department of Neurosurgery, Rezekne Hospital, Latvia

[108] Department of Anaesthesia, Critical Care & Pain Medicine NHS Lothian & University of Edinburg, Edinburgh, UK

[109] Director, MRC Biostatistics Unit, Cambridge Institute of Public Health, Cambridge, UK

[110] Department of Physical Medicine and Rehabilitation, Oslo University Hospital/University of Oslo, Oslo, Norway

[111] Division of Orthopedics, Oslo University Hospital, Oslo, Norway

[112] Institue of Clinical Medicine, Faculty of Medicine, University of Oslo, Oslo, Norway

[113] Broad Institute, Cambridge MA Harvard Medical School, Boston MA, Massachusetts General Hospital, Boston MA, USA

[114] National Trauma Research Institute, The Alfred Hospital, Monash University, Melbourne, Victoria, Australia

[115] Department of Neurosurgery, Odense University Hospital, Odense, Denmark

[116] International Neurotrauma Research Organisation, Vienna, Austria

[117] Klinik für Neurochirurgie, Klinikum Ludwigsburg, Ludwigsburg, Germany

[118] Division of Biostatistics and Epidemiology, Department of Preventive Medicine, University of Debrecen, Debrecen, Hungary

[119] Department Health and Prevention, University Greifswald, Greifswald, Germany

[120] Department of Anaesthesiology and Intensive Care, AUVA Trauma Hospital, Salzburg, Austria

[121] Department of Neurology, Elisabeth-TweeSteden Ziekenhuis, Tilburg, the Netherlands

[122] Department of Neuroanesthesia and Neurointensive Care, Odense University Hospital, Odense, Denmark

[123] Department of Neuromedicine and Movement Science, Norwegian University of Science and Technology, NTNU, Trondheim, Norway

[124] Department of Physical Medicine and Rehabilitation, St.Olavs Hospital, Trondheim University Hospital, Trondheim, Norway

[125] Department of Neurosurgery, University of Pécs, Pécs, Hungary

[126] Division of Neuroscience Critical Care, John Hopkins University School of Medicine, Baltimore, USA

[127] Department of Neuropathology, Queen Elizabeth University Hospital and University of Glasgow, Glasgow, UK

[128] Dept. of Department of Biomedical Data Sciences, Leiden University Medical Center, Leiden, The Netherlands

[129] Department of Pathophysiology and Transplantation, Milan University, and Neuroscience ICU, Fondazione IRCCS Cà Granda Ospedale Maggiore Policlinico, Milano, Italy

[130] Department of Radiation Sciences, Biomedical Engineering, Umeå University, Umeå, Sweden

[131] Perioperative Services, Intensive Care Medicine and Pain Management, Turku University Hospital and University of Turku, Turku, Finland

[132] Department of Neurosurgery, Kaunas University of Health Sciences, Kaunas, Lithuania

[133] Intensive Care and Department of Pediatric Surgery, Erasmus Medical Center, Sophia Children's Hospital, Rotterdam, The Netherlands

[134] Department of Neurosurgery, Kings college London, London, UK

[135] Neurologie, Neurochirurgie und Psychiatrie, Charité – Universitätsmedizin Berlin, Berlin, Germany

[136] Department of Intensive Care Adults, Erasmus MC– University Medical Center Rotterdam, Rotterdam, the Netherlands

[137] icoMetrix NV, Leuven, Belgium

[138] Movement Science Group, Faculty of Health and Life Sciences, Oxford Brookes University, Oxford, UK

[139] Psychology Department, Antwerp University Hospital, Edegem, Belgium

[140] Director of Neurocritical Care, University of California, Los Angeles, USA

[141] Department of Neurosurgery, St.Olavs Hospital, Trondheim University Hospital, Trondheim, Norway

[142] Department of Emergency Medicine, University of Florida, Gainesville, Florida, USA

[143] Department of Neurosurgery, Charité – Universitätsmedizin Berlin, corporate member of Freie Universität Berlin, Humboldt-Universität zu Berlin, and Berlin Institute of Health, Berlin, Germany

[144] VTT Technical Research Centre, Tampere, Finland

[145] Section of Neurosurgery, Department of Surgery, Rady Faculty of Health Sciences, University of Manitoba, Winnipeg, MB, Canada